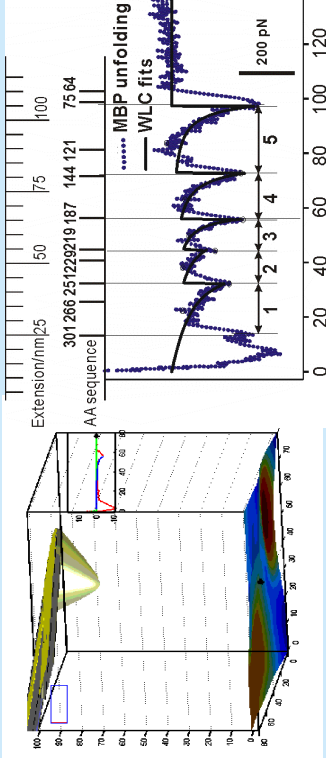


NRC-CNRC

*Steele Institute
for Molecular
Sciences*

Mechanical Unfolding of Single Proteins and AFM-based Force Mapping



Shan Zou

Biomolecular Sensing and Imaging
100 Sussex Drive, Ottawa, ON, K1A 0R6

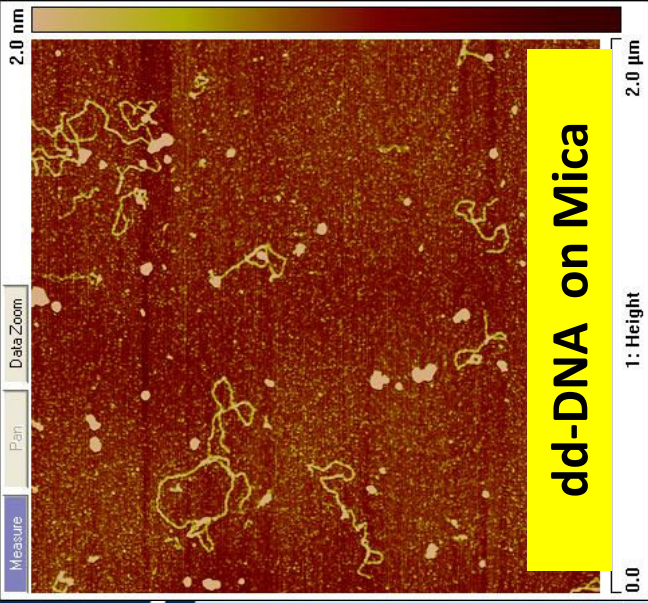
shan.zou@nrc.ca



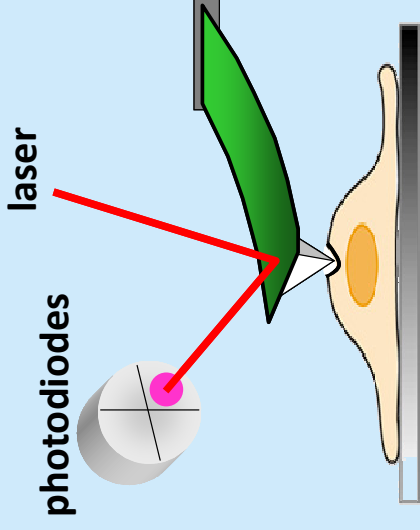
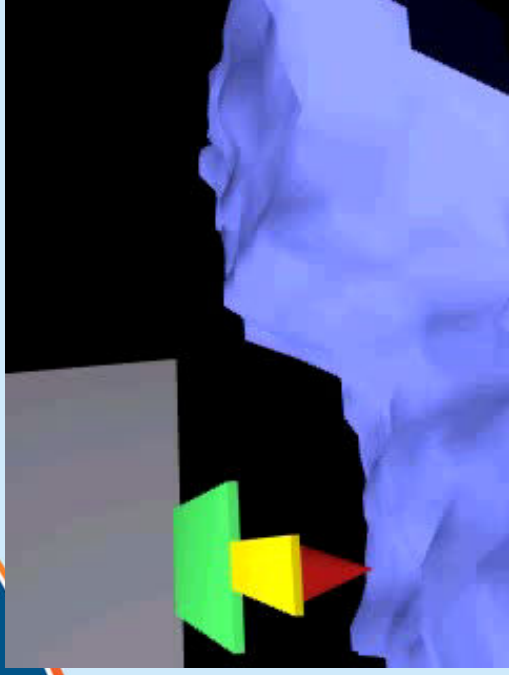
National Research
Council Canada

Conseil national
de recherches Canada

Canada

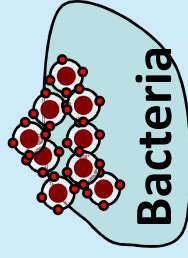
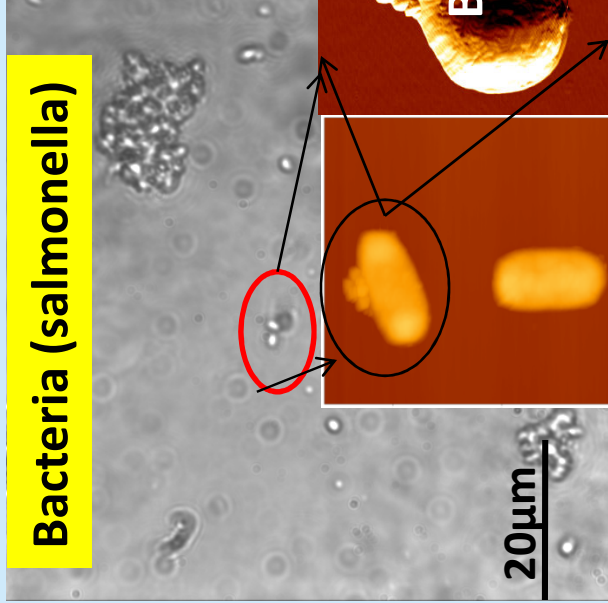


Atomic Force Microscopy (AFM)

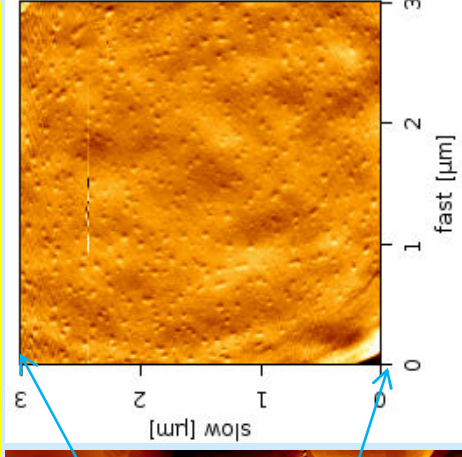
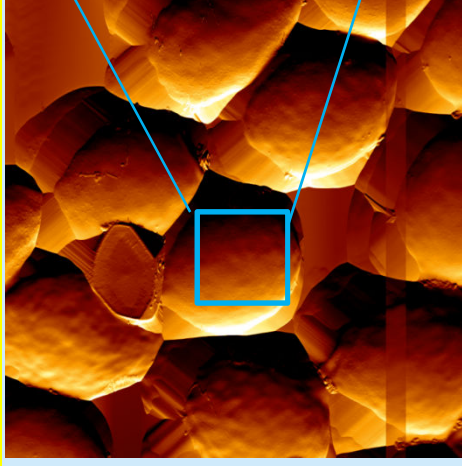


High spatial resolution!

Bacteria (salmonella)



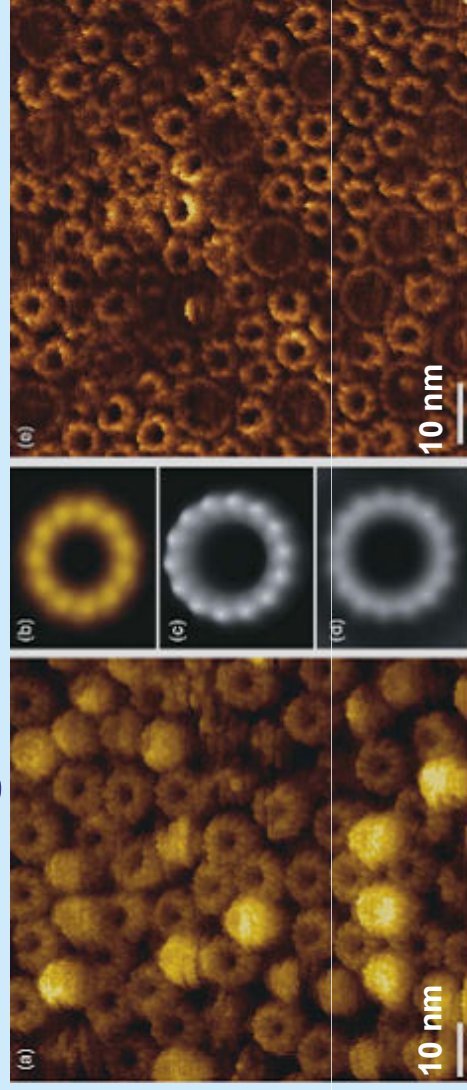
Yeast cells exposed to Se nanoparticles



~60 nm Nanoparticles were observed on the cell surfaces. (With Zoltan Mester, INMS)

With C. Paquet(SIMS) , and S. Ryan, J. Tanha (IBS)

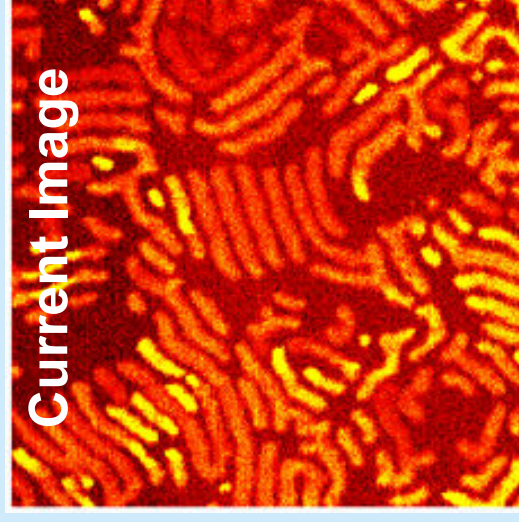
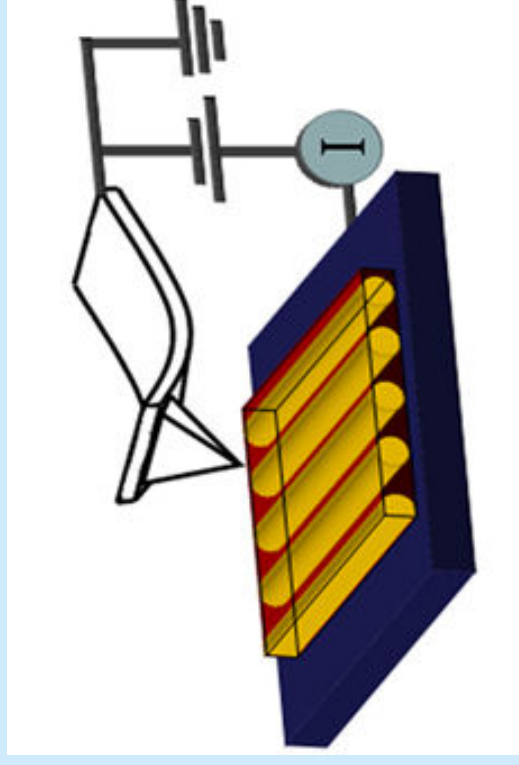
High Resolution AFM



Oligomeric assemblies of native membrane proteins by AFM. (a) Topography (raw data) of sodium-driven rotors from FoF1-ATP synthases of *Ilyobacter tartaricus*. Averaged topographs of ion-driven rotors from FoF1-ATP synthases of (b) *I. tartaricus*, (c) spinach chloroplasts and (d) *Spirulina platensis*; (e) The raw data AFM image of a core complex surrounded by seven peripheral antenna (LH2) complexes to the structural model derived from it.

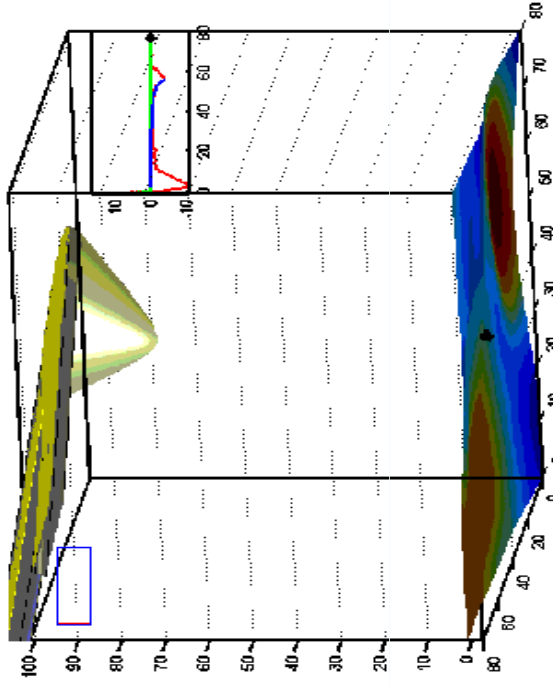
Scheuring S. and Sturgis J. (2005) Science 309, 484-487

Conductive Probe AFM

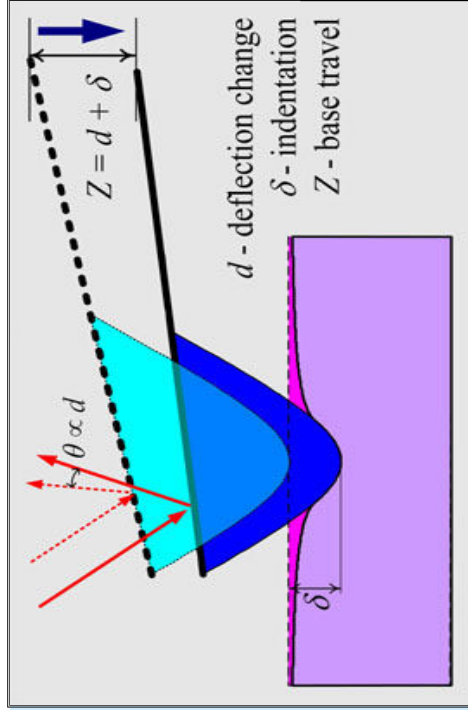
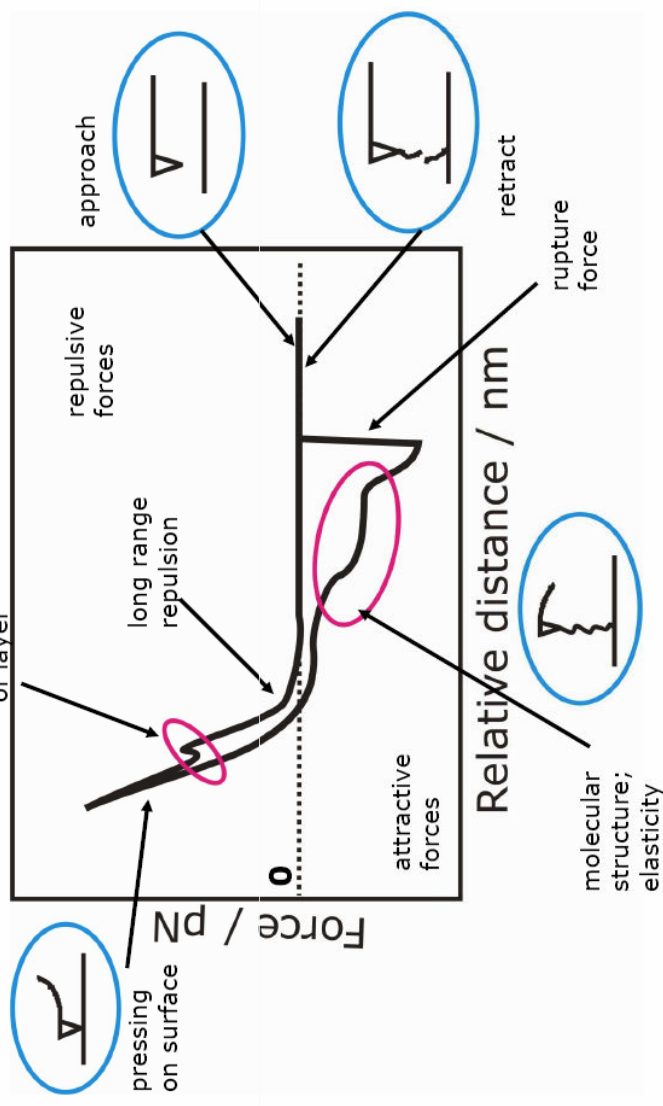


NRC Canada, University of Toronto, University of Bristol
Li JK; Zou S; Rider D; Manners I; Walker GC *Adv. Mater.* 2008, 20, 1989-1993.
Wang YS, Zou S, Winnik MA, Manners I *Chemistry Eur. J.* 2008, in press.

AFM-based Single Molecule Force Spectroscopy (SMFS)

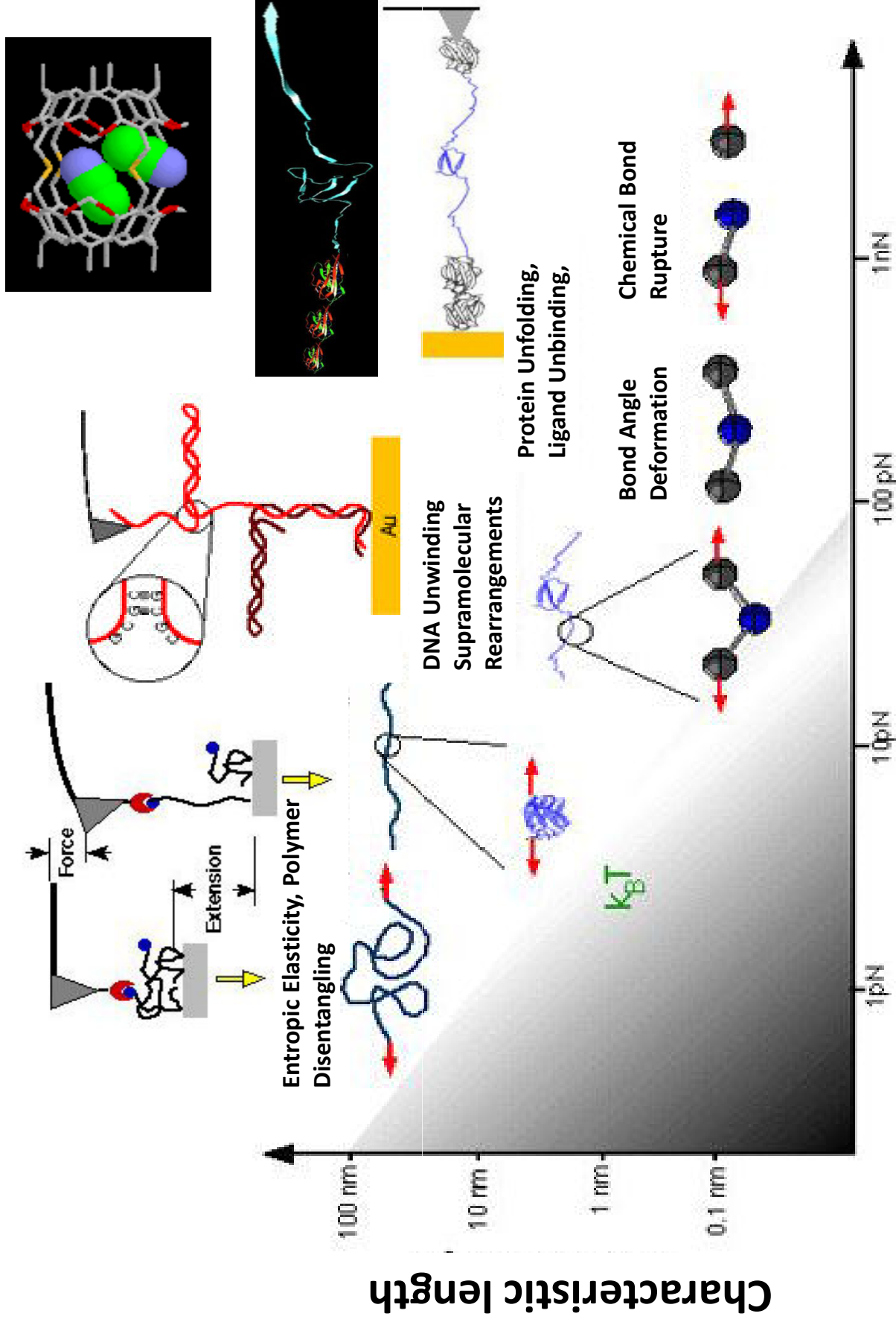


Interpretation of force-distance curves

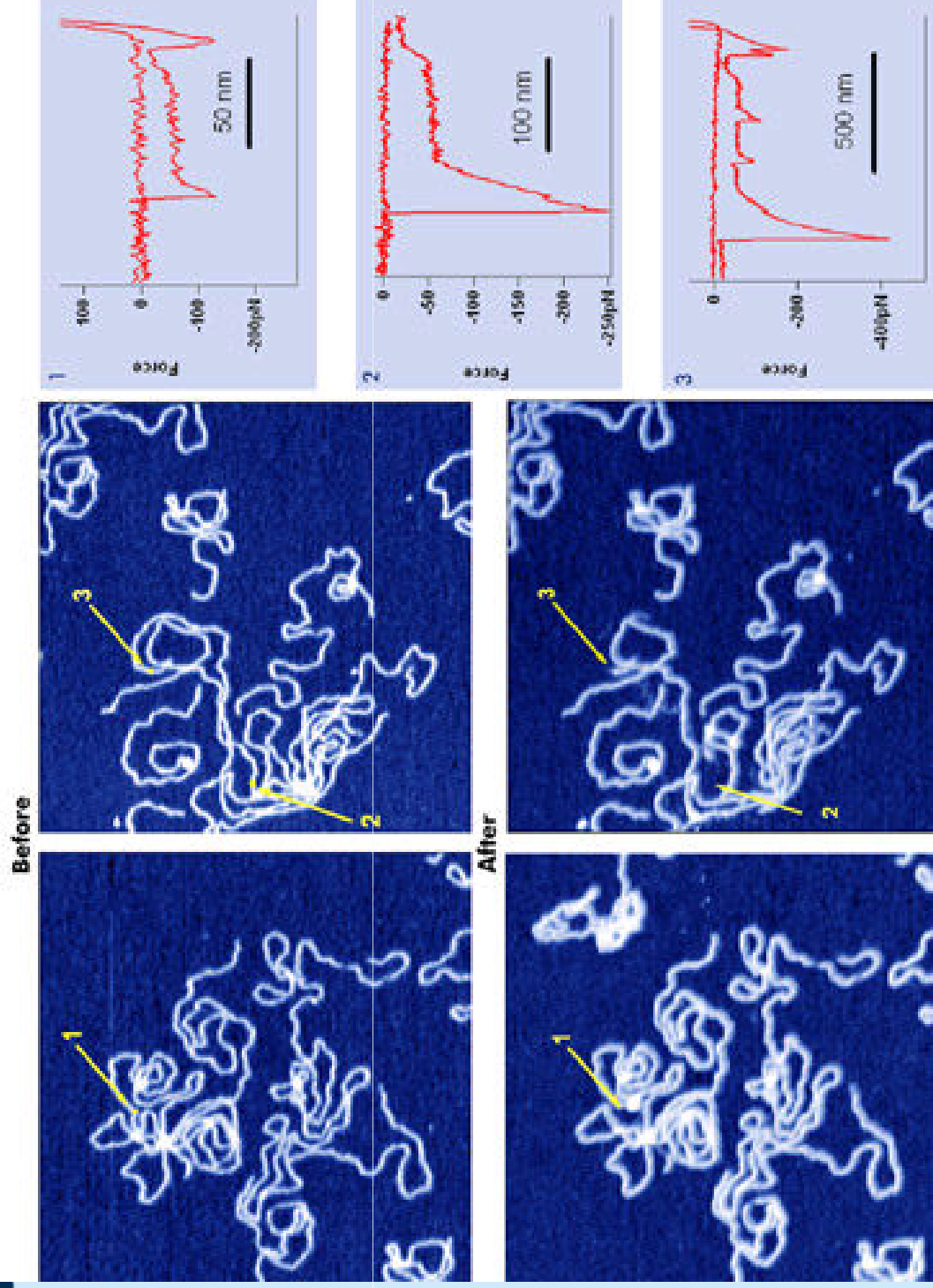


$$F = \frac{4E\sqrt{R}}{3(1 - \sigma^2)} \delta^{3/2}$$

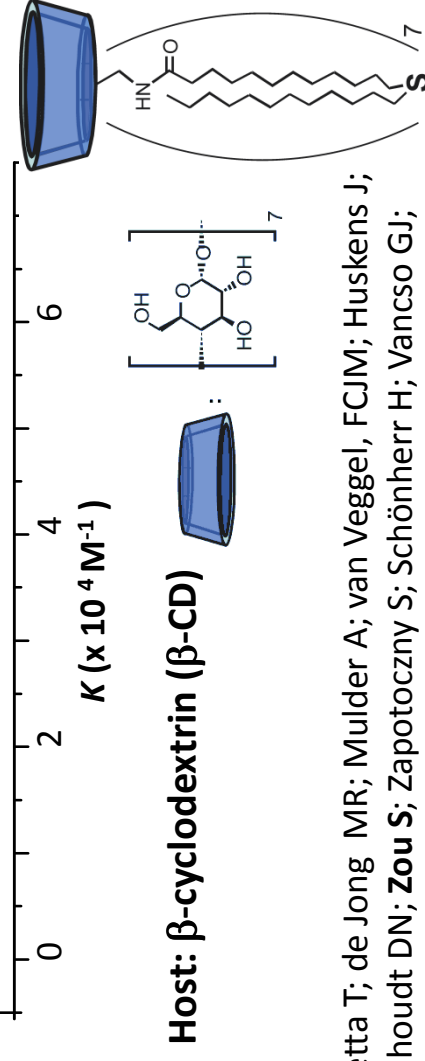
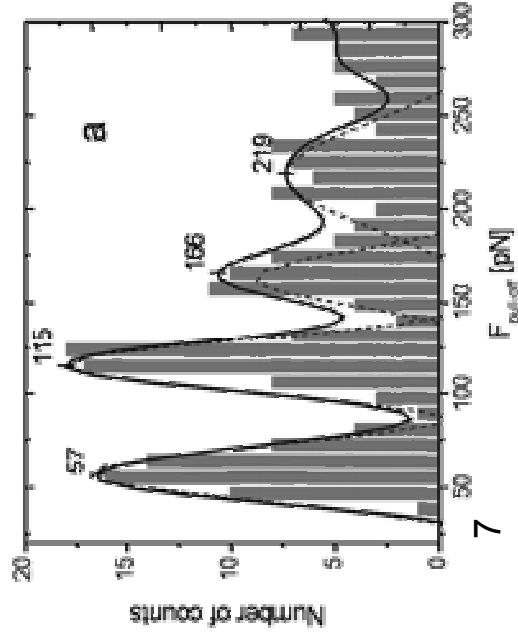
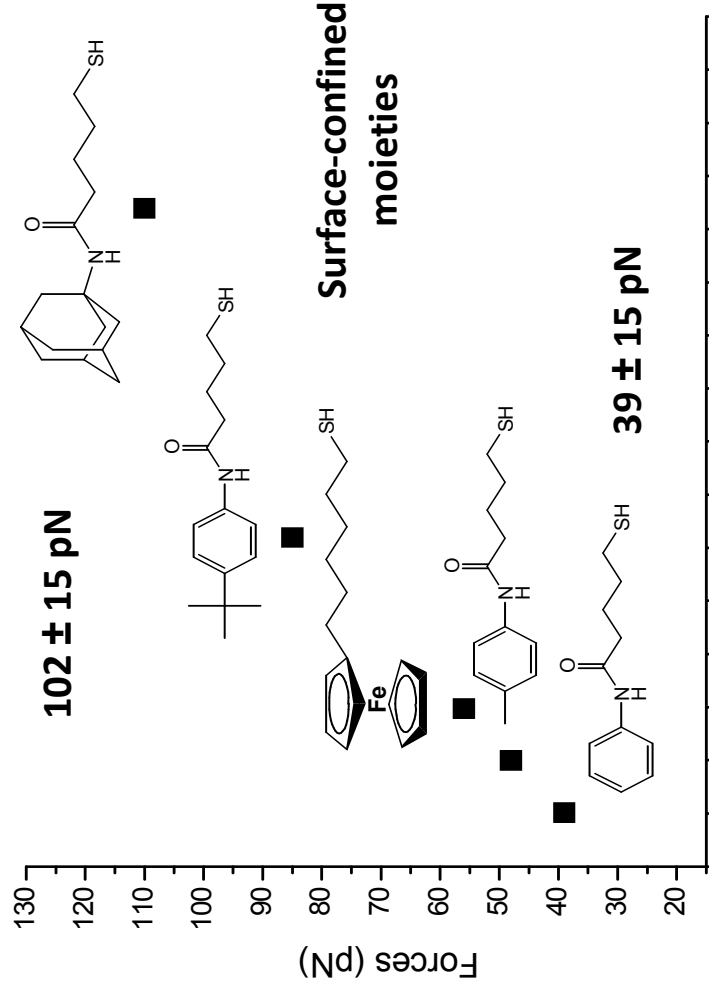
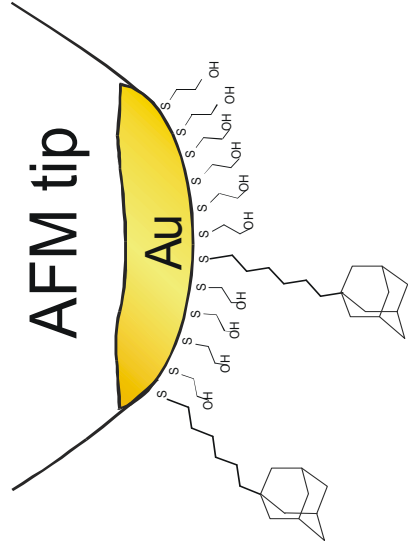
Stretching & Interaction Forces by SMFS



Unzipping of single double stranded DNA molecules by SMFS

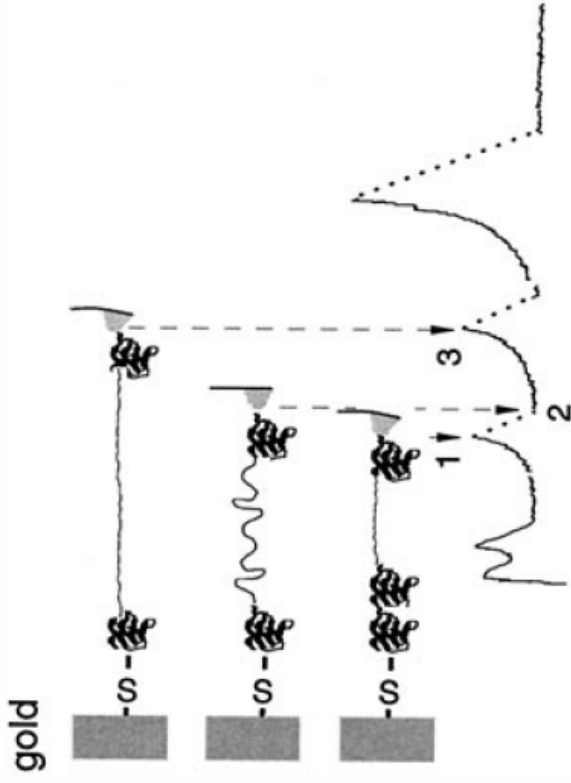


Host-Guest (ligand-receptor) Interactions

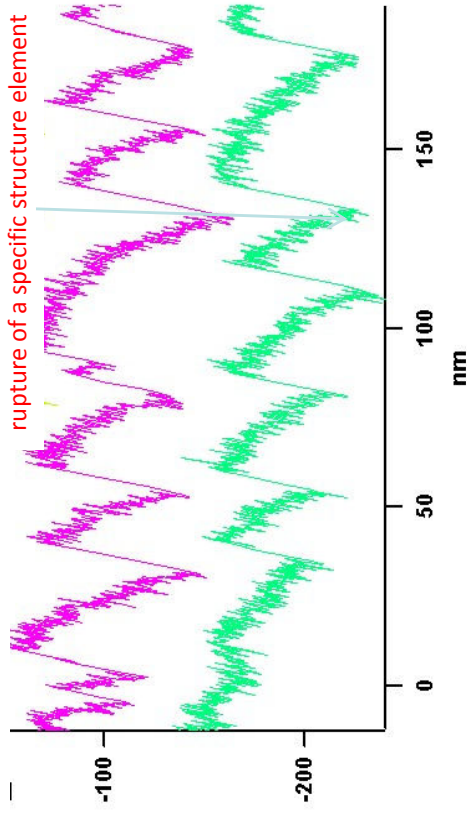


Auletta T; de Jong MR; Mulder A; van Veggel, FCJM; Huskens J;
 Reinhoudt DN; Zou S; Zapotoczny S; Schönherr H; Vancso GJ;
 Kuipers L *J. Am. Chem. Soc.*, 2004, 126, 1577.
 Zou, S.; et.al. *Langmuir*, 2003, 19, 8618.
 Zou, S.; et.al. *Angew. Chem. Int. Ed.* 2005, 44, 956-959.
 Zou, S.; et.al. *J. Am. Chem. Soc.*, 2005, 127, 11230.

Mechanical Unfolding of Adhesion Proteins



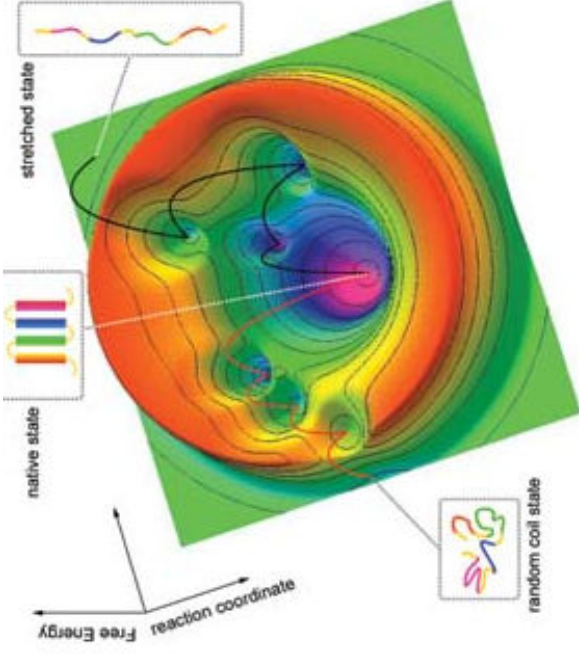
Bovine Fibronectin III, Titin



Single modules of multi-domain **adhesion proteins** unfold in a largely **two-state manner**. The forced unfolding of each domain is initiated by the rupture of a specific structure element (most commonly secondary structure), which leads to rapid unfolding of the whole domain into a random coil chain.

Exposing the protein to heat or chemical denaturants is the classical way of driving a protein out of its folded conformation through this energy landscape to an unfolded conformation (red pathway). However, the exact pathway of mechanical unfolding or reaction coordinate is not necessary the same (black pathway).

A funnel-shaped energy landscape



MECHANICAL denaturation of non-mechanical protein???



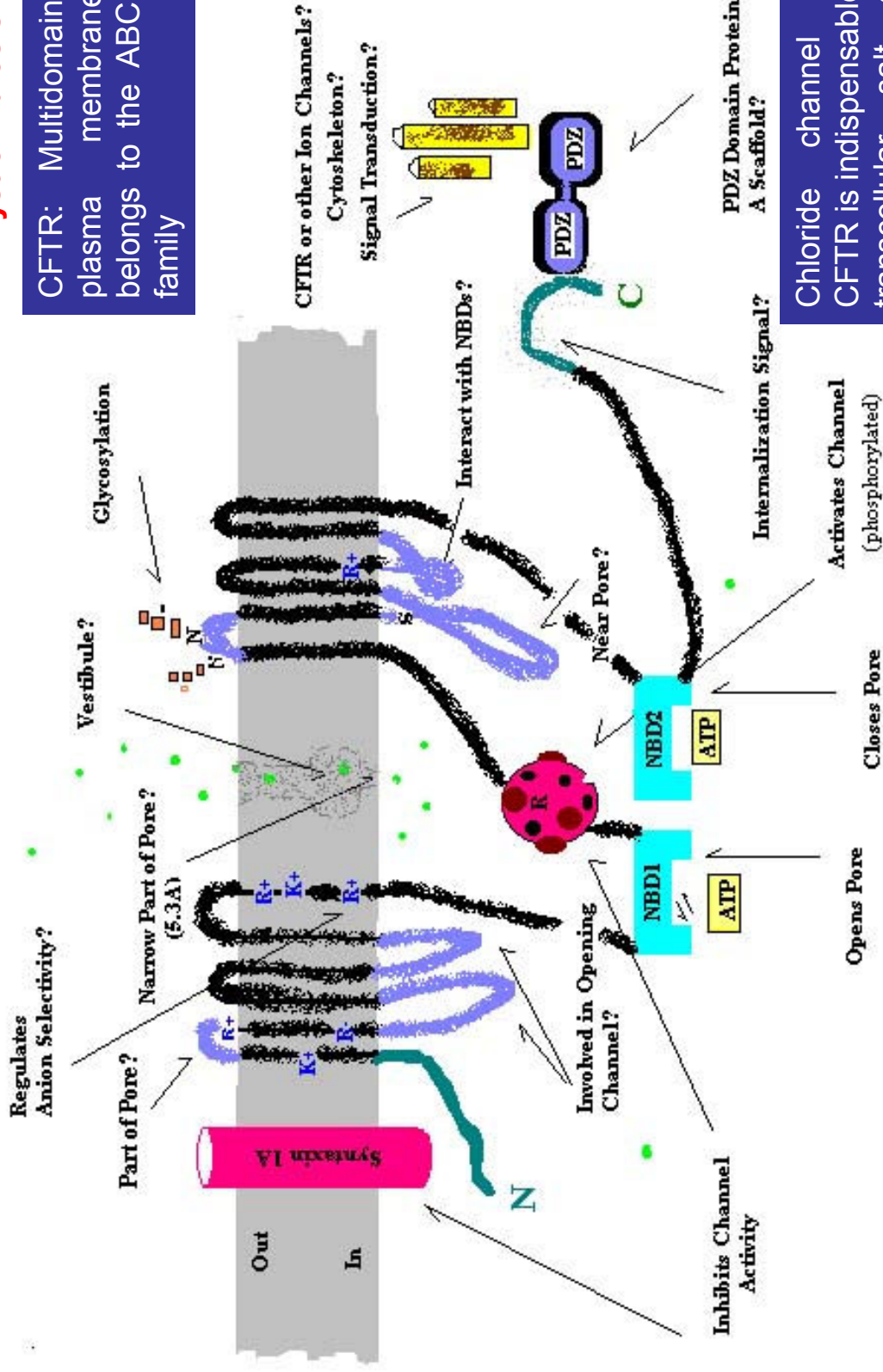
Single Molecule Study on STRUCTURAL TRANSITIONS

Specifically, how much the typical two-state behavior in thermal/salt induced denaturation of MBP would be preserved in mechanical denaturation?

Characterization of NBD1 and NBD2-MBP of CFTR by Integrated AFM, Confocal FL and Single-Molecule Force Spectroscopy

Collaboration with G. C. Walker, G. Lukacs,
University of Toronto, Sick Children Hospital, McGill University
Cystic Fibrosis Foundation

CFTR: Multidomain, polypeptidic plasma membrane protein; belongs to the ABC transporter family

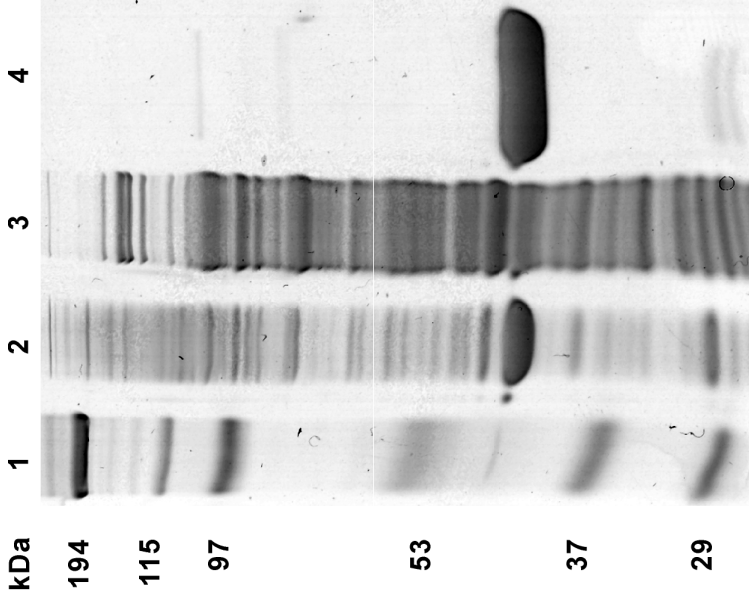


Chloride channel activity of CFTR is indispensable for normal transcellular salt and water transport in numerous organs.

http://www2.montana.edu/cftr/PointandClick/putting_it_all_together.htm

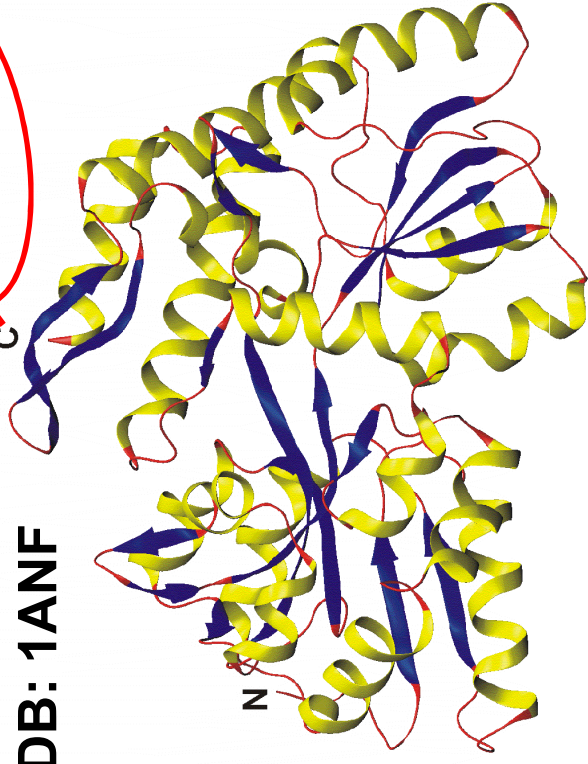
Maltose Binding Protein (MBP)

14% SDS PAGE stained with Coomassie Brilliant Blue R250: Lane 1 –Marker, Lane 2 – Supernatant, Lane 3 – Pellet, Lane 4 – Eluted MBP protein.



Well expressed in the bacteria cytoplasm and was found to be a single two-state unfolding transition upon *heating*.

PDB: 1ANF



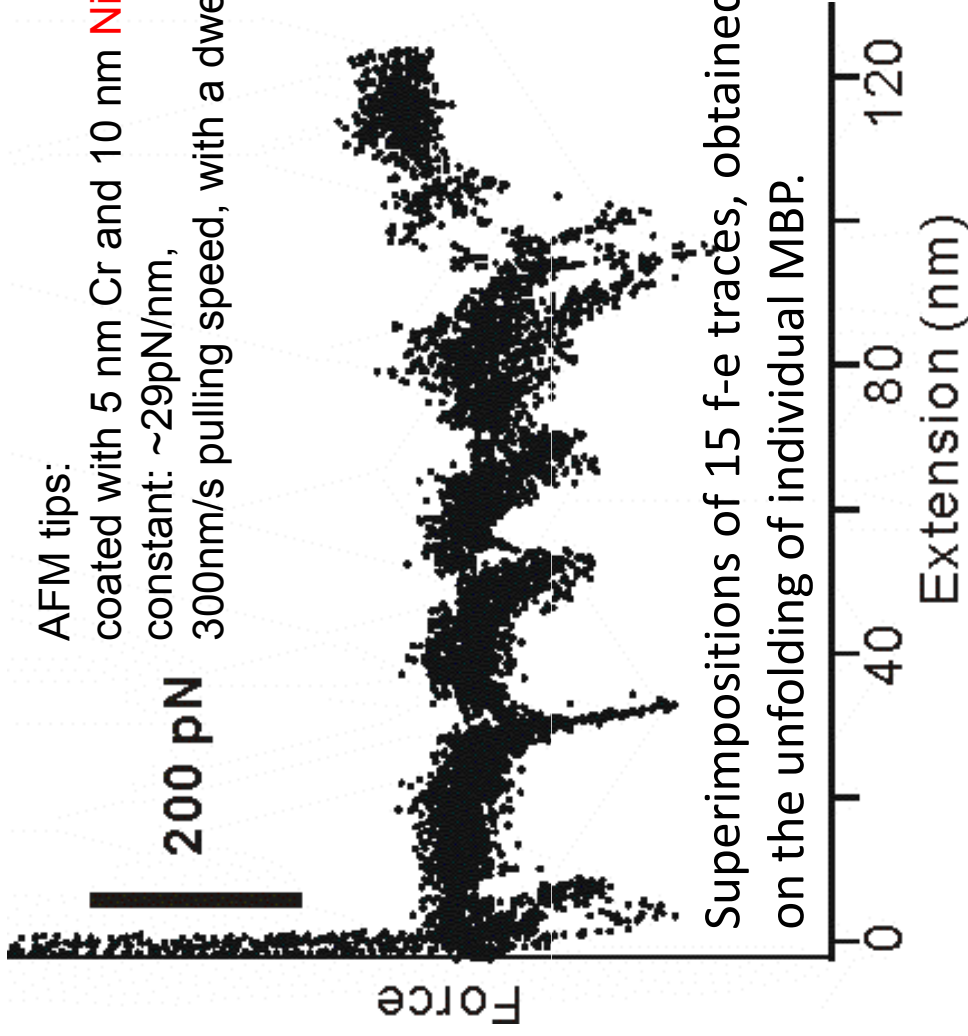
MBP source: in the periplasm of *Escherichia coli*. – responsible for catabolism of maltodextrin

Widely used as solubilizing agent – generate affinity handles for purification of recombinant proteins

number of Residues: 366
beta-strands: 23; alpha helices: 16

in our study: C terminus modified with 6 His-tags

Unfolding of Single MBP Molecules



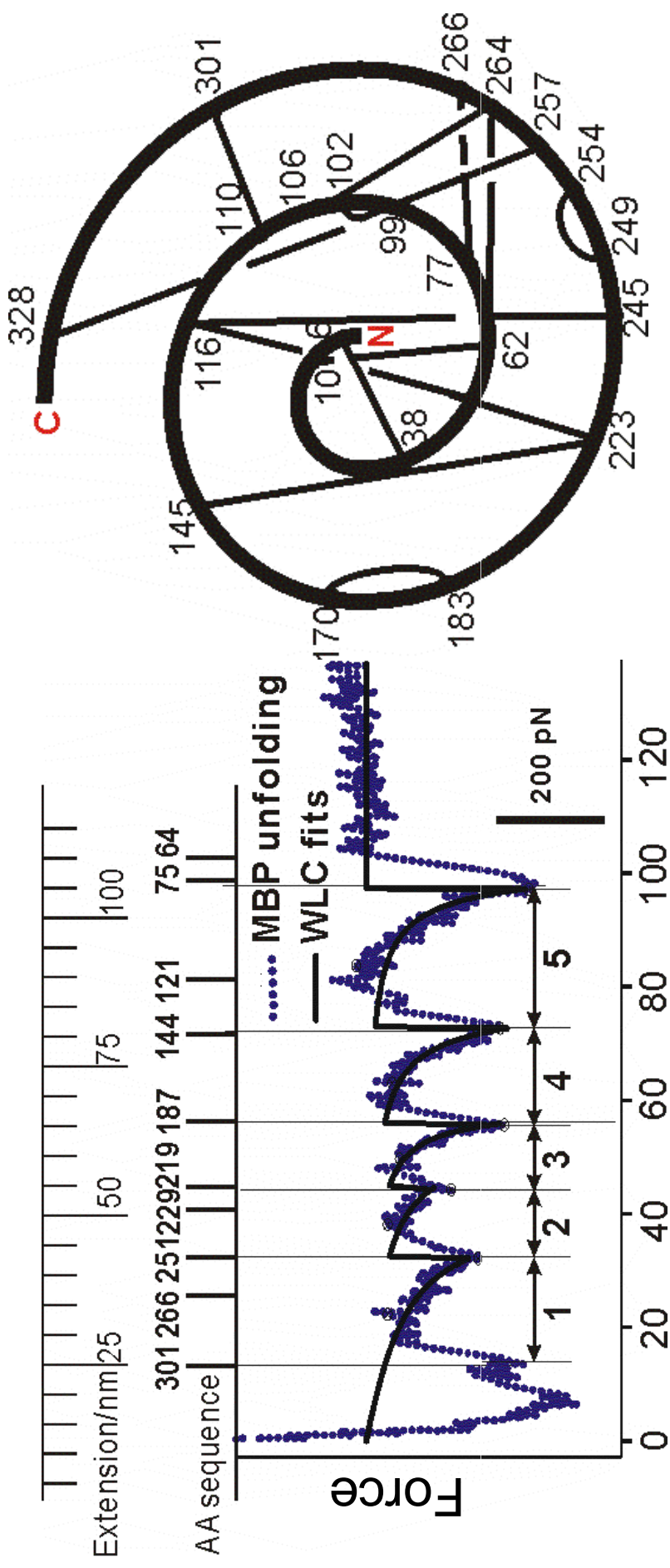
AFM tips:
coated with 5 nm Cr and 10 nm Ni; spring
constant: ~29pN/nm,
300nm/s pulling speed, with a dwell time of 2 s .

- Six His-tags at C-terminus improve the attachment probability of MBP to Ni-AFM tips by 30 %.
- Common unfolding patterns were highlighted in the denser regions by alignment of the f-e curves.

- **MULTIPLE force transitions → mechanical unfolding of MBP is not two-state, but multiple states.**

Demonstrate that force is not projected along the “thermal” denaturation coordinate.

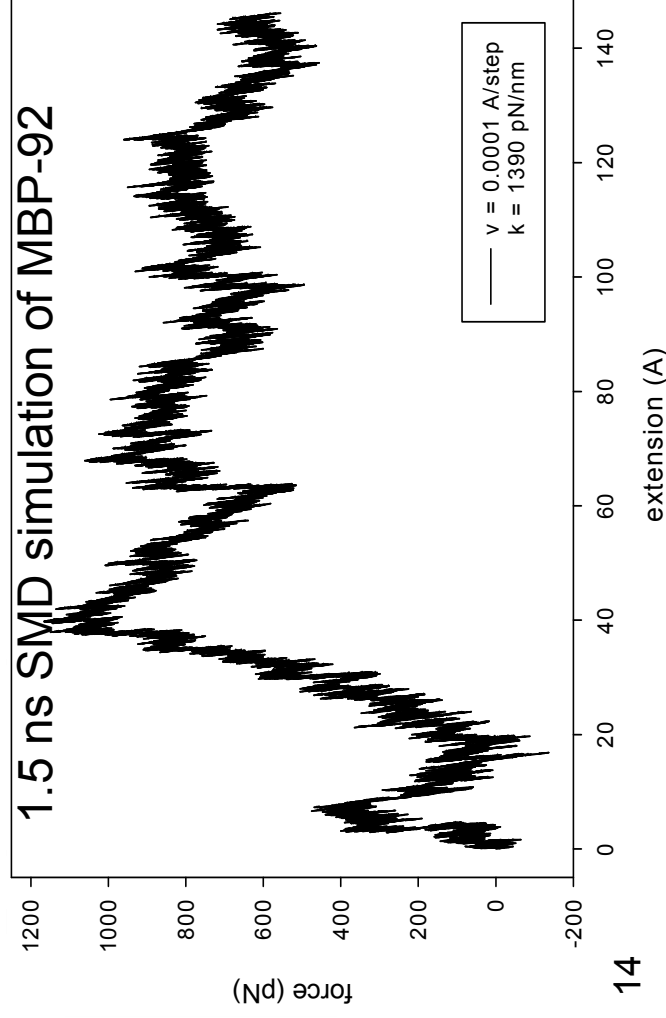
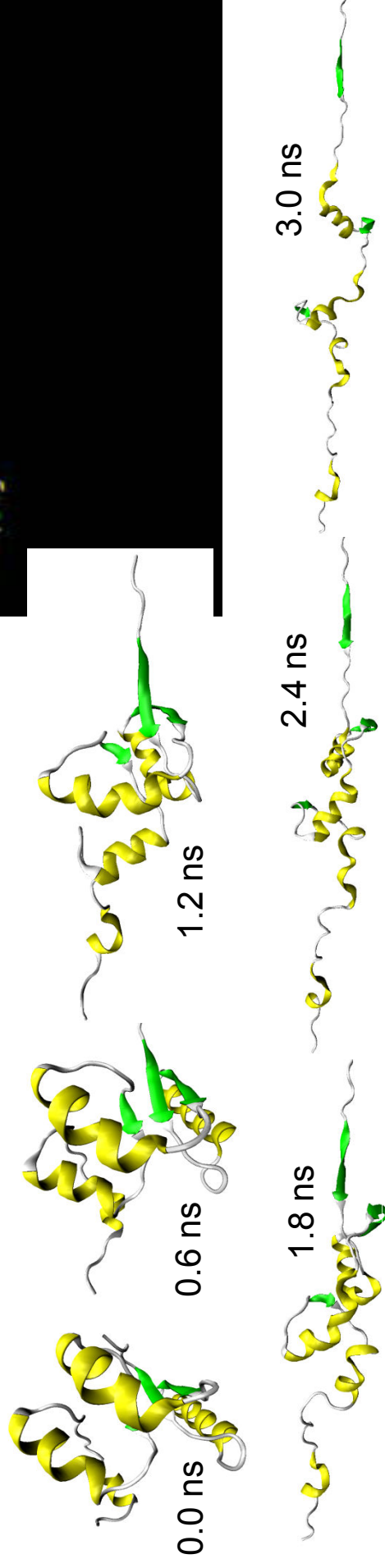
Unfolding of Single MBP Molecules



The sequential unfolding events of the MBP only occur at the ends of beta-sheet regions, suggesting that cooperative interactions exist between two neighbouring secondary beta strands within a single protein molecule.

MD Simulation Data

First 92 residues fragment :



The force peak occurs at 40 Å corresponding to the middle beta strand breaking away from the top strand, but still connected to the bottom one. The next one at 75 Å is attributed to the separating of this beta strand from the lower one.

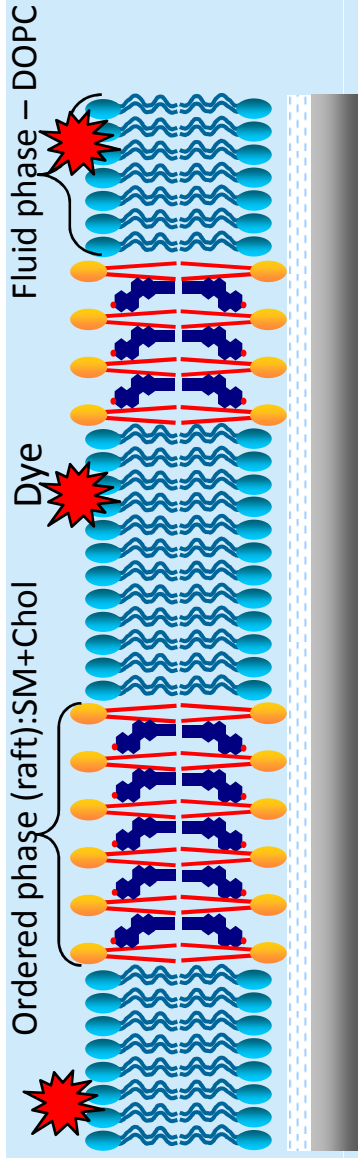
For MBP-92 -- seen unfold sequentially rather than in a two-state process; -- seen that a “core” of stable structure remained until the full unfolding occurred.

Membrane Restructuring

Collaboration with Dr. Linda J. Johnston

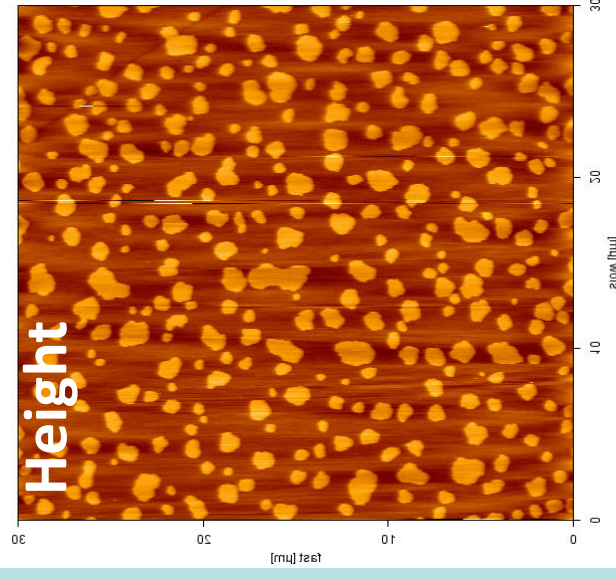
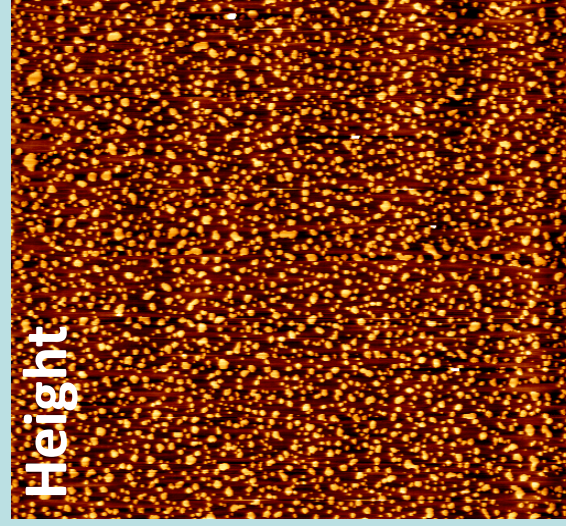
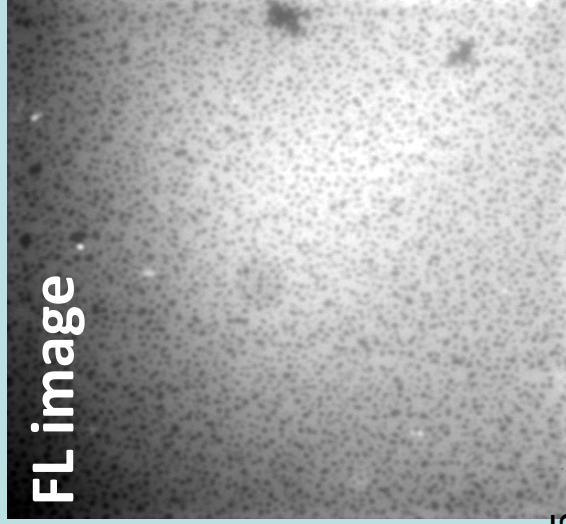
Induced by Enzymatic Generation of Ceramide using Integrated AFM and Fluorescent Microscopy

DOPC(TRO.3%): Egg Sphingomyelin: Cholesterol (DEC 2:2:1)

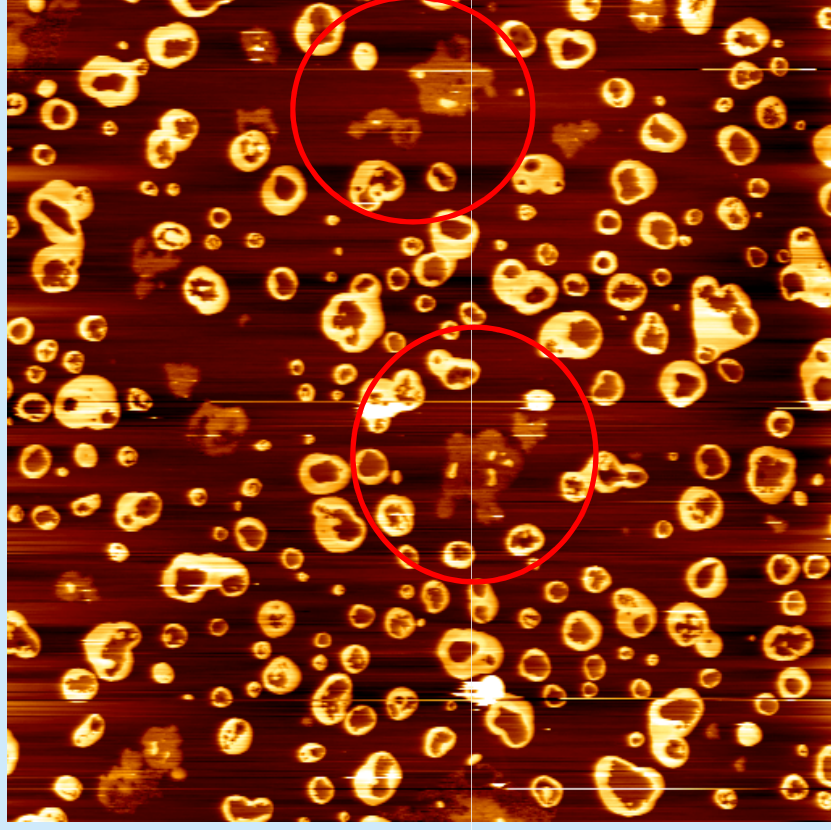
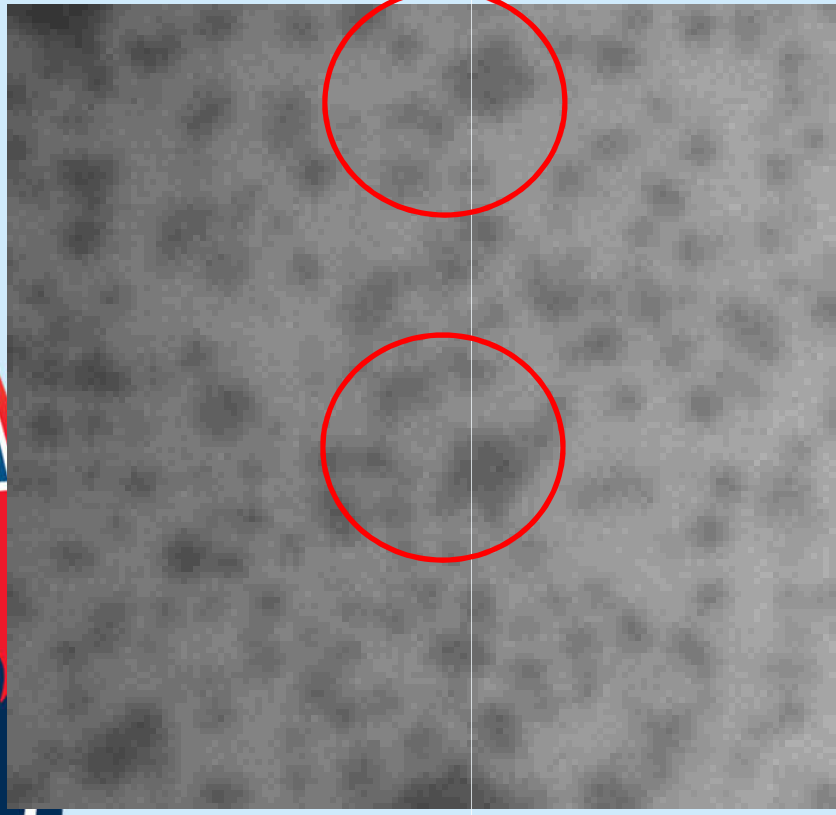


Ceramide involved as a messenger in signaling during Apoptosis cell differentiation and growth suppression.

→ Restructuring of the cell membrane lipids.

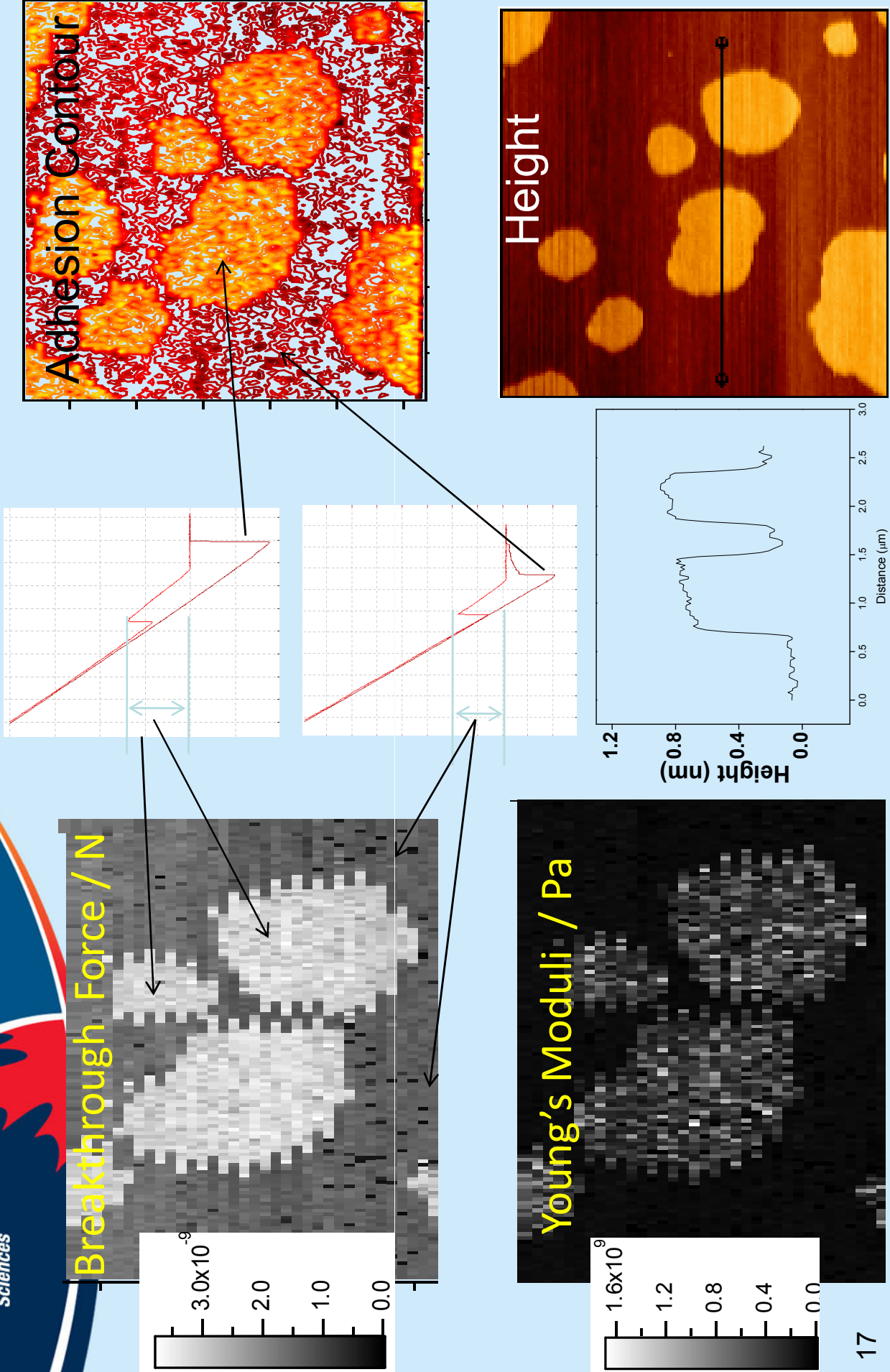


Relevant to SMase-mediated changes to raft domains in cellular membranes

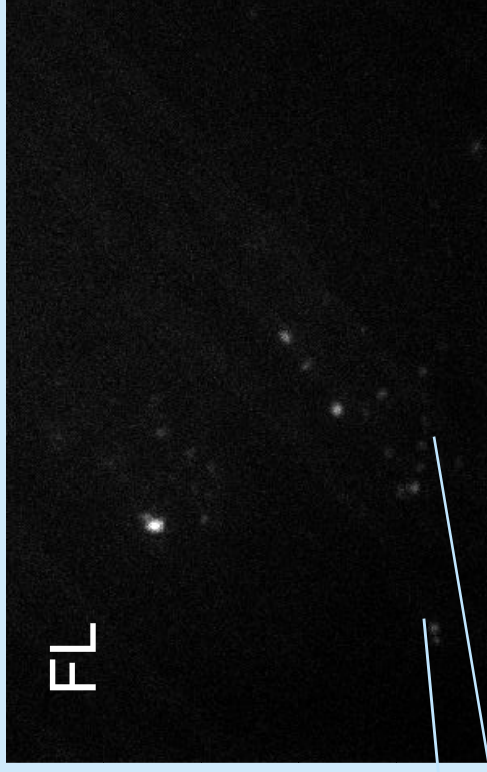


- Dye-excluded regions initially formed adjacent to liquid-ordered domains and grew to large patches that included a number of initial domains.
 - AFM showed that ceramide generation led to heterogeneous domains with many small higher regions of a ceramide-enriched phase.
 - Ceramide generation leads to cholesterol expulsion from the domains, generating cholesterol enriched regions in the surrounding DOPC phase that excludes dye and has decreased fluidity.
- 16 Direct visualization for cholesterol expulsion from liquid-ordered domains in response to ceramide production.

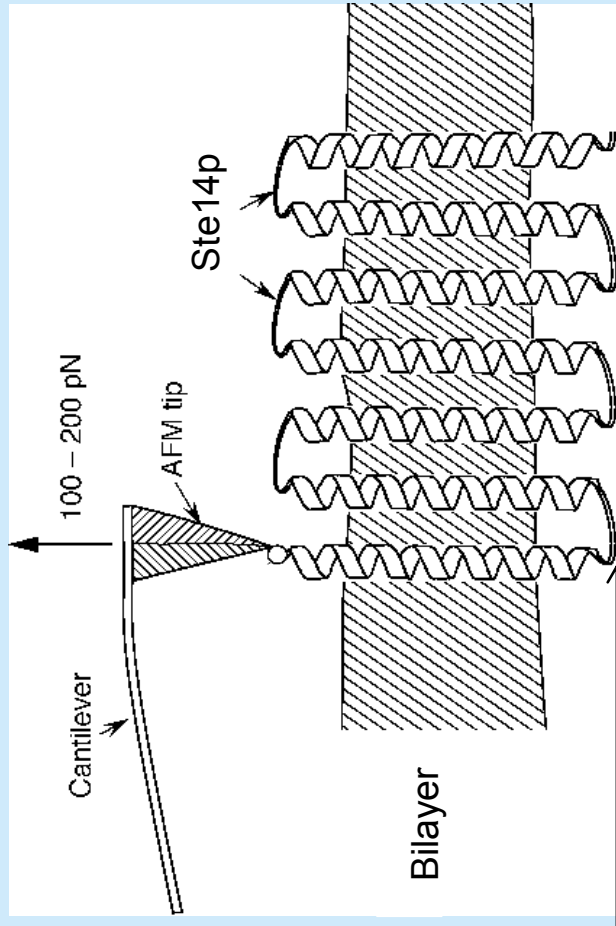
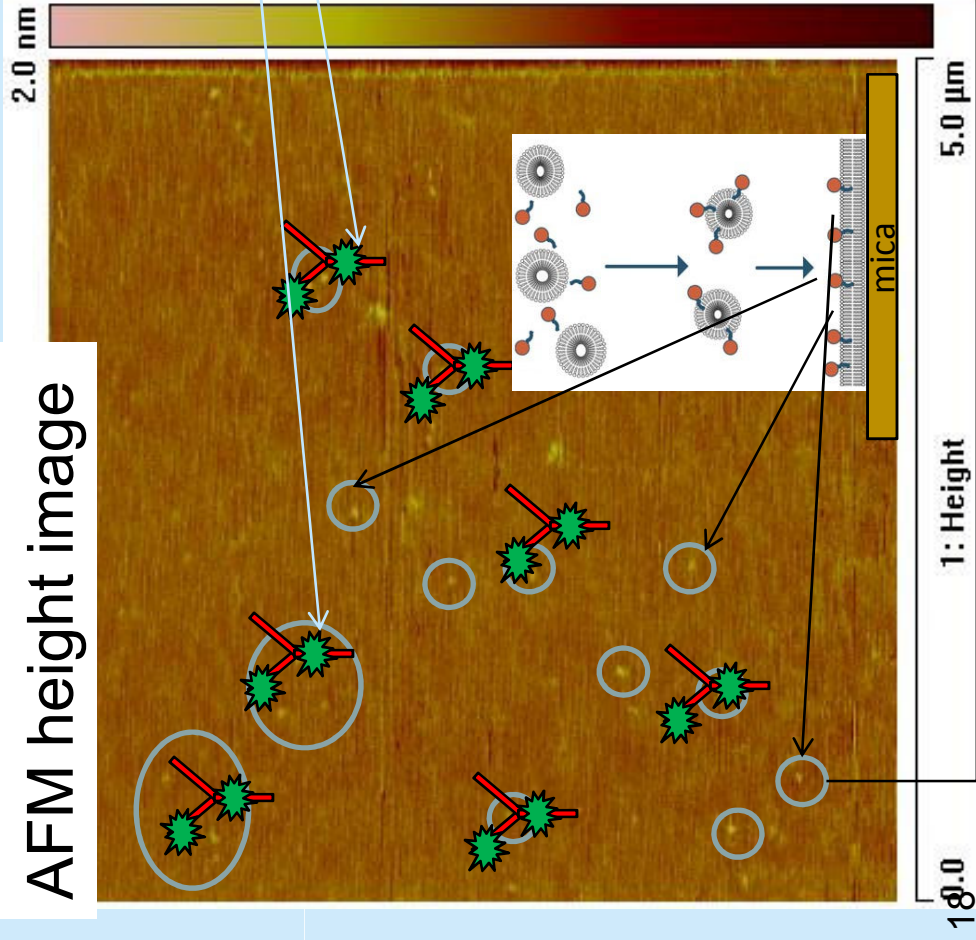
Force mapping



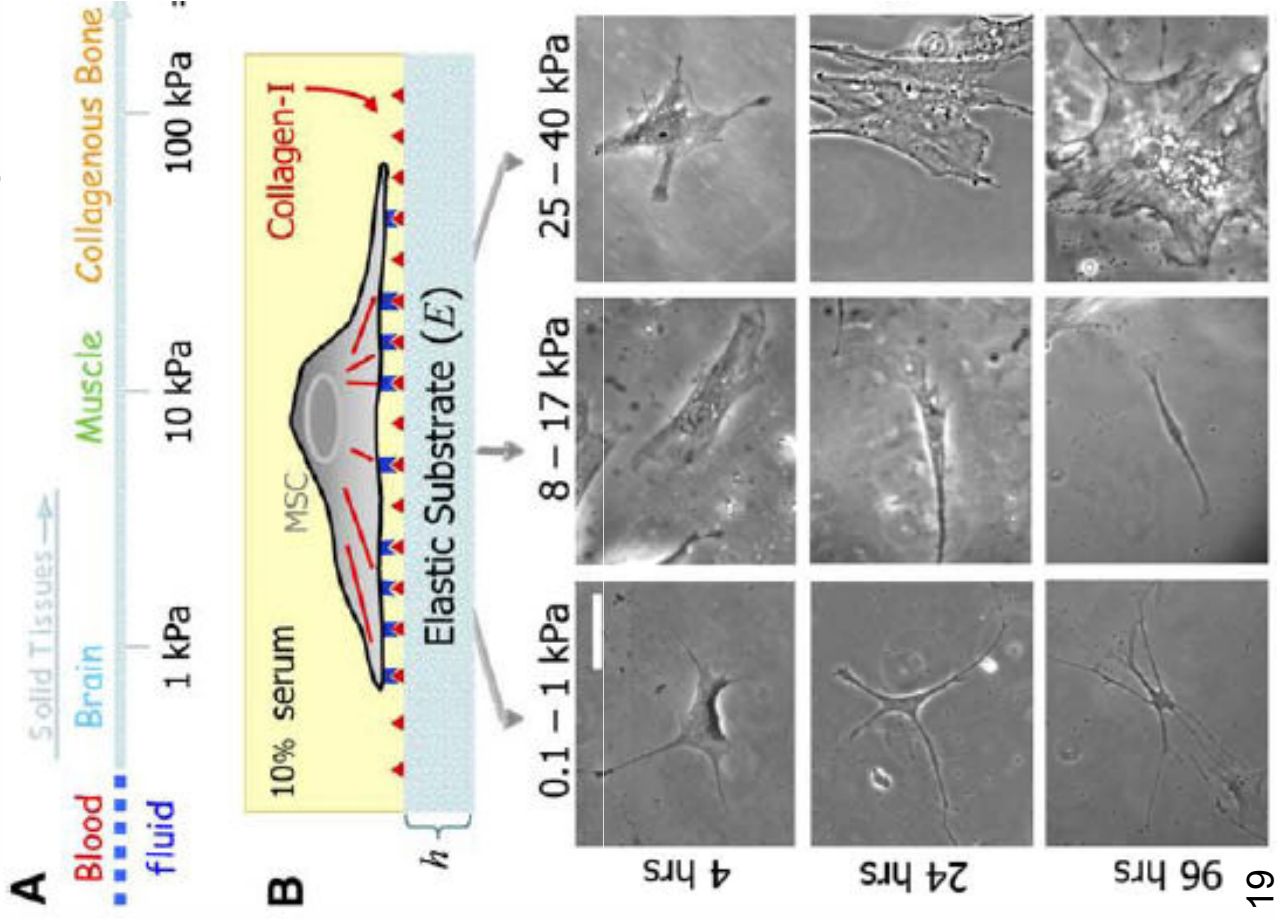
Membrane Protein Interaction by Multimodal Techniques



AFM height image



Matrix Elasticity Directs Stem Cell Lineage



Microenvironments appear important in stem cell lineage specification.

Naive mesenchymal stem cells (MSCs) are shown here to specify lineage and commit to phenotypes with extreme sensitivity to tissue level elasticity.

AFM was used for Matrix Elasticity and Cell Mechanics Measurements.

The results have significant implications for understanding physical effects of the in vivo microenvironment and also for therapeutic uses of stem cells.

DE Discher Cell (2006) 126, 677.

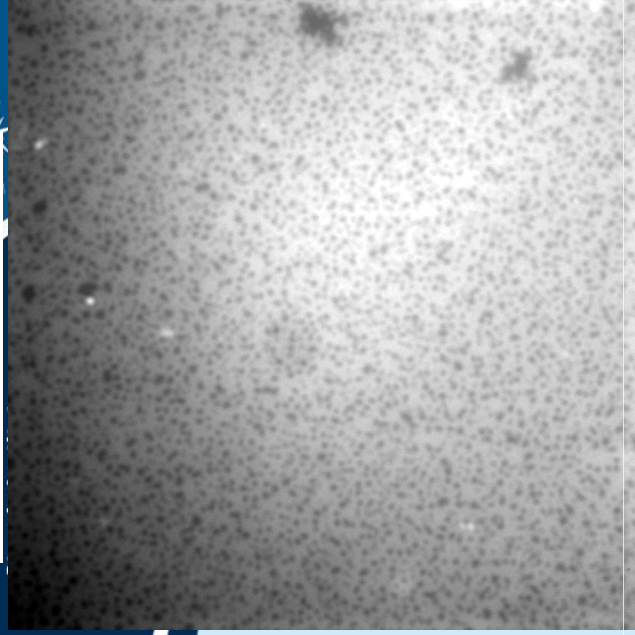
AFM-based SMFS is Capable of:

- nanometer scale features of biological samples in physiological-like environment.
- dynamical events (protein folding-unfolding) at nanometer scale resolution.
- nano-mechanical properties of living cells.

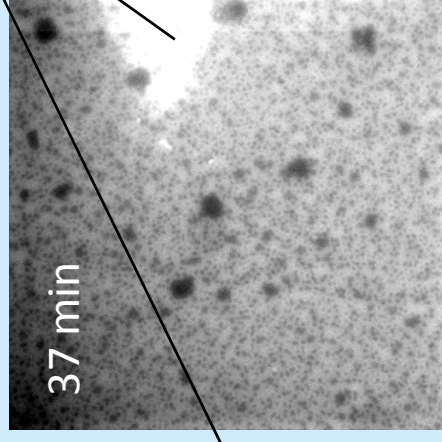
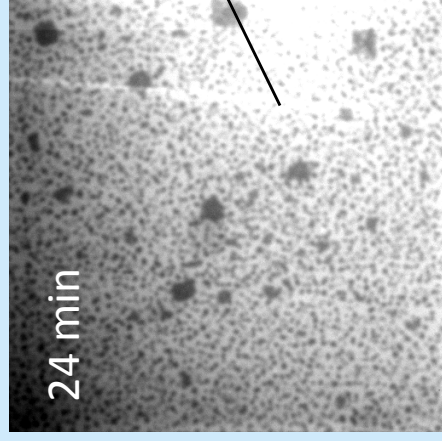
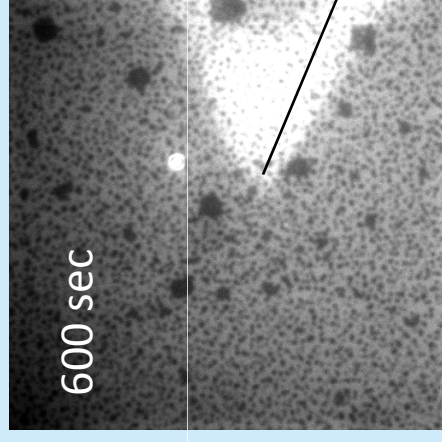
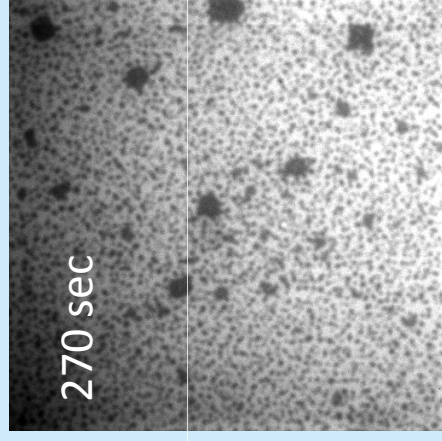
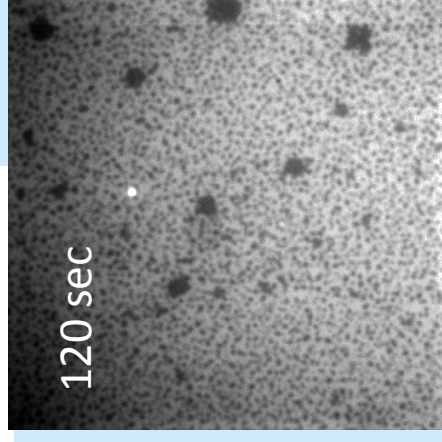
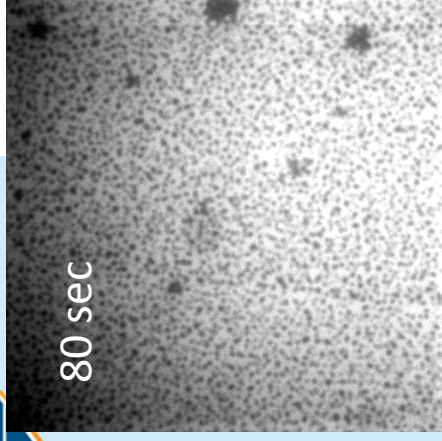
Thank you for your attention!



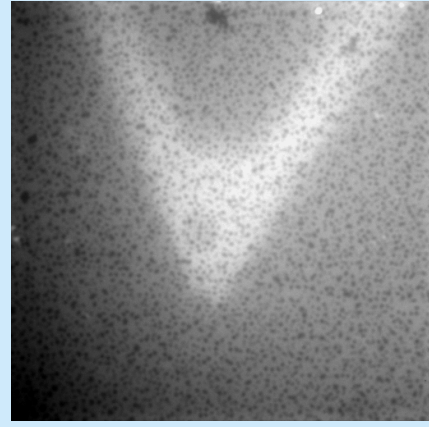
Before SMase



After SMase



Dye-excluded regions initially formed adjacent to liquid-ordered domains and grew to large patches that included a number of initial domains.



ARC1000

St
fo
Sc

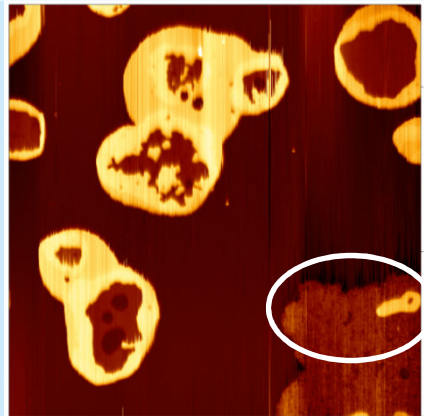
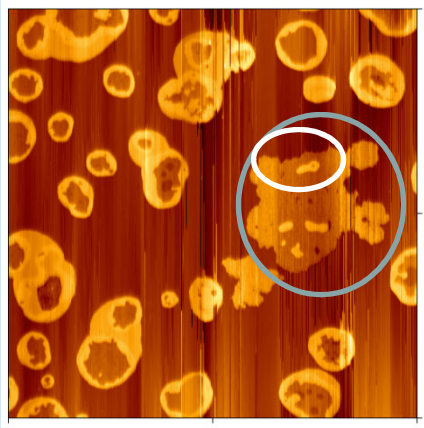
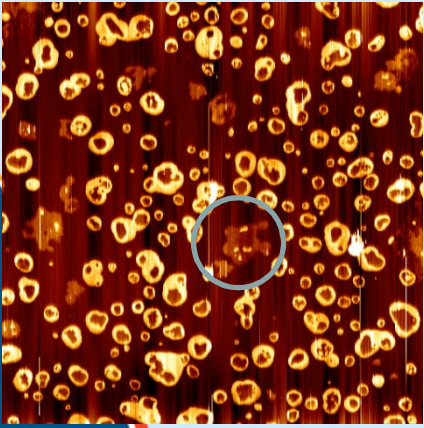
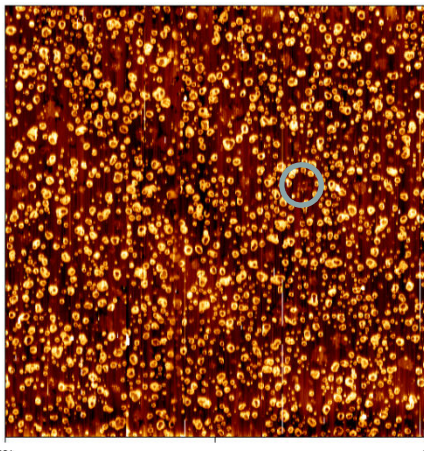
100 μm X 100 μm

30 μm X 30 μm

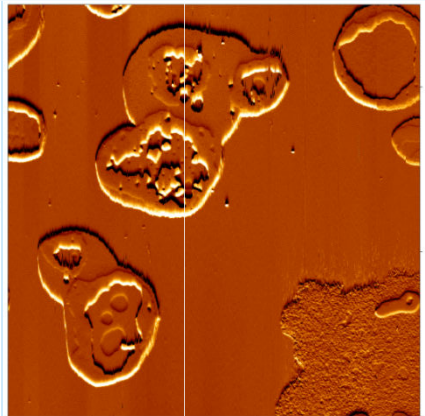
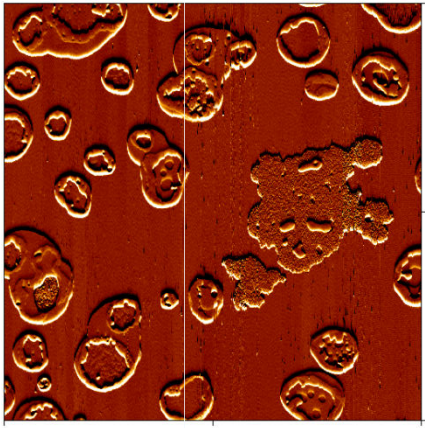
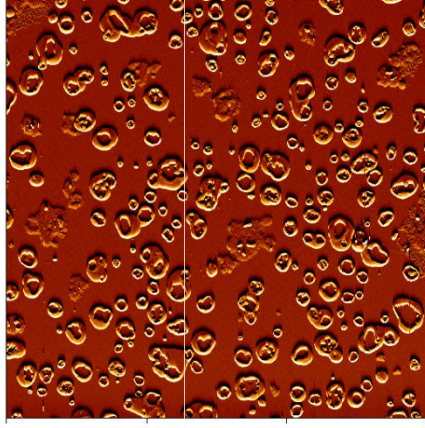
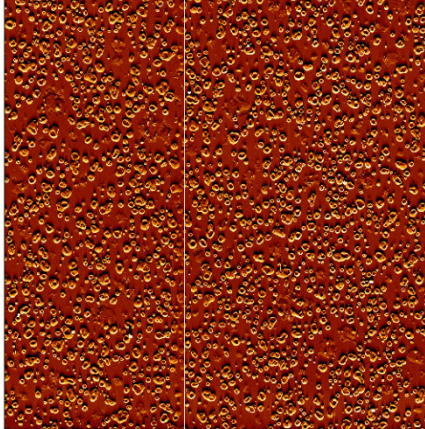
10 μm X 10 μm

5 μm X 5 μm

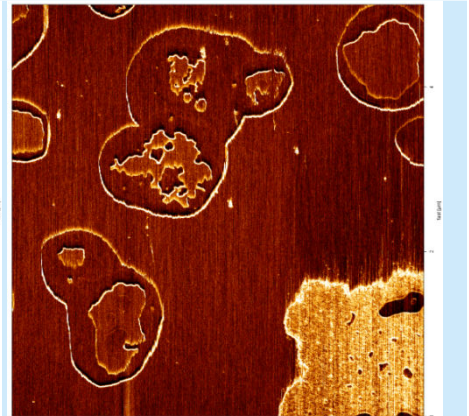
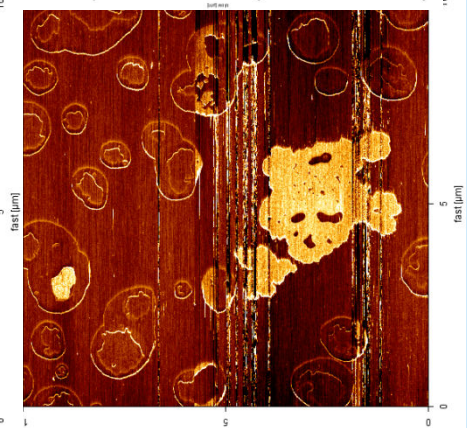
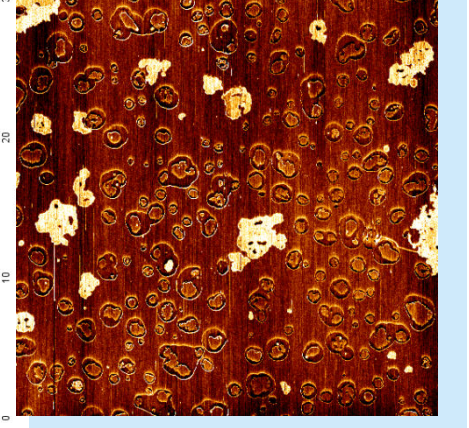
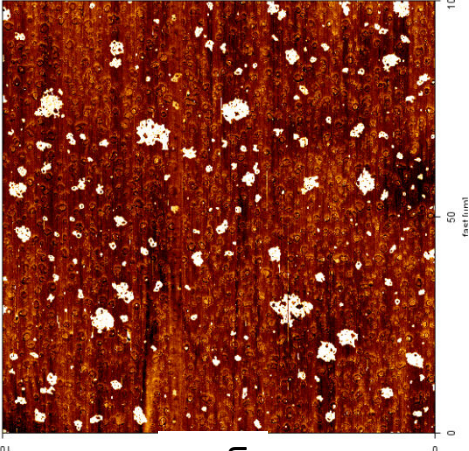
Height



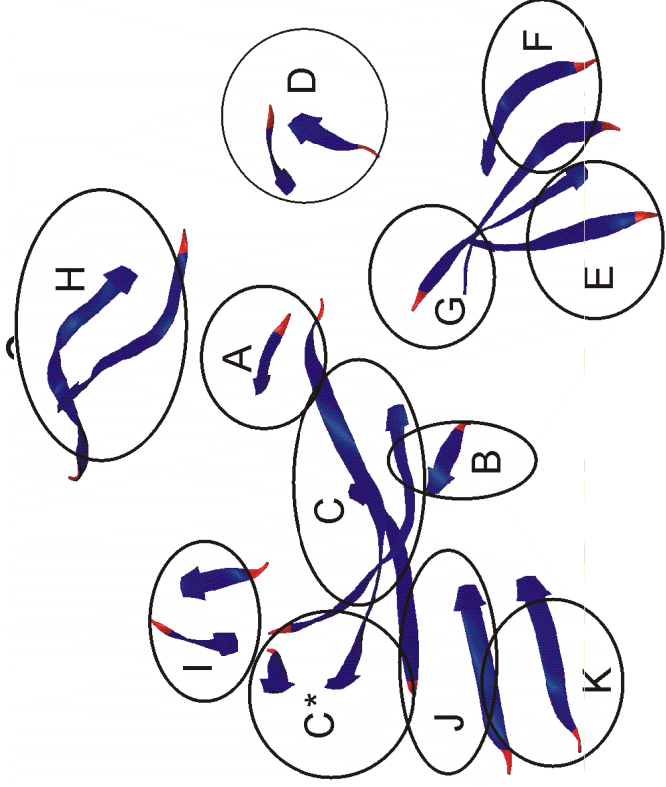
Vertical deflection



Lateral deflection



Sequential Unfolding of MBP



Well match → β sheets unfold as groups of secondary structure.

Note that this does not imply that the β -strand hydrogen bond cleavages necessarily initiate at the ends of β -sheet regions, since the cantilever probes with a minimum time constant of 100 microseconds – all chain dynamics within that time period are integrated into a single response. Transitions associated with groups of alpha helical structure are not observed, which indicates that beta sheet structures of MBP are more resistant to mechanical unfolding than those alpha helical structures.

Extension (nm)	25	38	43	54	66	81	90	106	109								
Assigned positions	301	265	251	222	187	144	119	78	64								
β -strand ends	301	264	254	249	245	223	183	170	145	116	110	106	99	77	62	38	10
Division	0aa	1aa	2aa	-1aa	4aa	-1aa	3aa	1aa	2aa								

Maltose Binding Protein Unfolding

- Multiple unfolding force transitions observed in the unfolding experiments of single MBP molecules
- C terminus attachments destabilize secondary structure unit nearest to it, thus the unfolding starts from C terminus.

Funding from NSERC, Cystic Fibrosis Foundation, CRC

Probabilities of Force Transitions of MBP

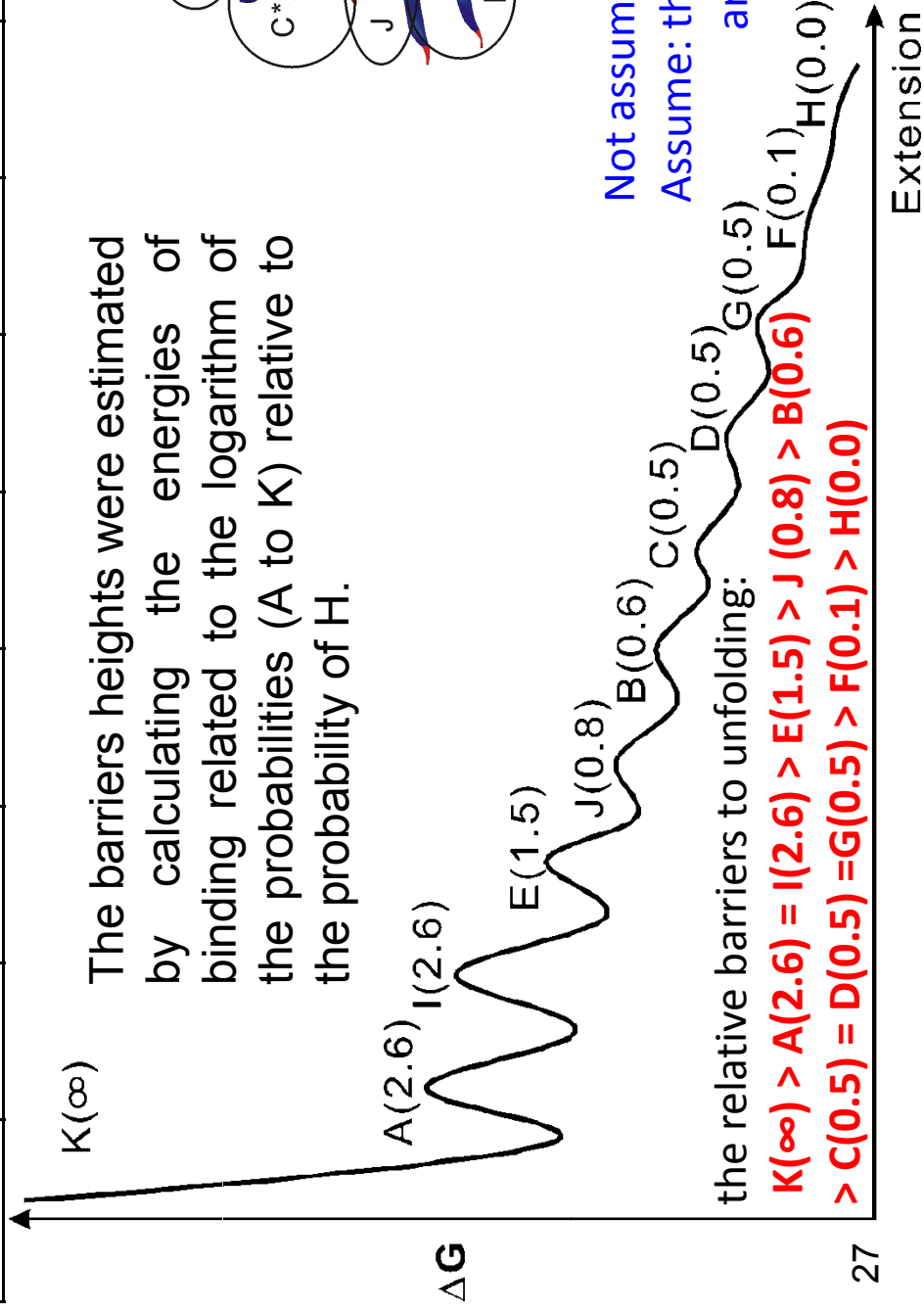
Beta sheet Curve name	A 328→257	B 301→110 266→77* 264→62*	C 264→106	D 254→249	E 245→116	F 223→145	G 223→116	H 183→170	I 102→99	J 62→10	K 38→9
C235		301	265	251	121	145	219	187		63	
1034 (339)						144		185			
78		310						187		65	
624		301				148	228	181		63	
67			78	251	119-116	144		188			
307				253			220	163		63	
618			78	247		145	220		102	60	
50			263-271			144		186			
417			259-269			145	222	174			
M636			266	249		144	222	185			
M1034 (338)		300		251	118	146		188			
M871				249(b)		145		193			(43)
M234 (345)		306	264			144	222	191		65	
M314	325	302	260			144	224				
M998 (340)		301		251				185			
probability	0.067	0.467	0.533	0.533	0.200	0.800	0.533	0.867	0.067	0.400	0

The barriers heights can be estimated by calculating the

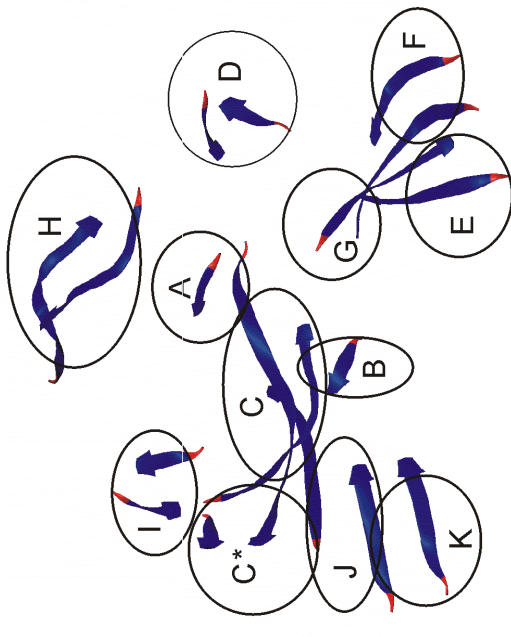
energies of binding related to the logarithm of the probabilities

Suggested Multiple Barrier-crossing Unfolding Process w/o Applied Forces

Beta sheet	A 328→257	B 301→110	C 264→106 266→77* 264→62*	D 254→249	E 245→116	F 223→145	G 223→116	H 183→170	I 102→99	J 62→10	K 38→9
probability	0.067	0.467	0.533	0.533	0.200	0.800	0.533	0.867	0.067	0.400	0

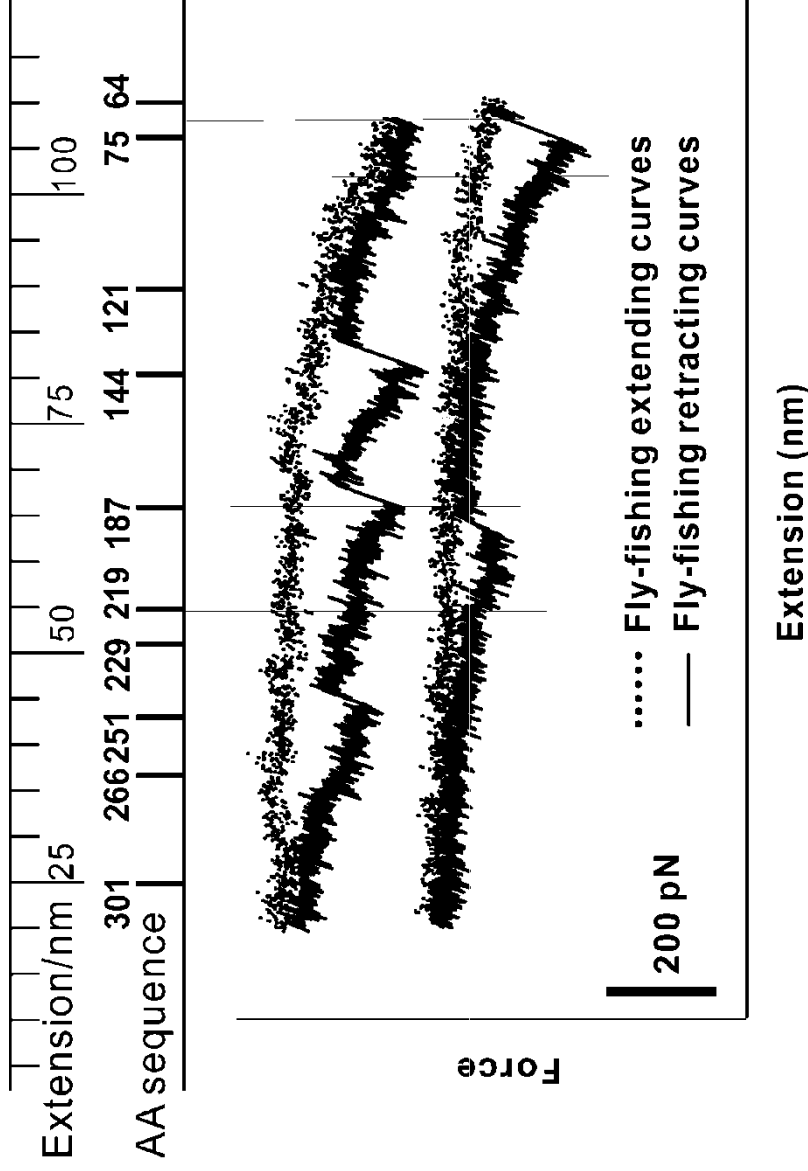


The barriers heights were estimated by calculating the energies of binding related to the logarithm of the probabilities (A to K) relative to the probability of H.



Not assuming: the protein is misfolded;
 Assume: the barrier heights to unfolding are close to $k_b T$ in energy.

Unfolding and Refolding of MBP – “flying fishing”

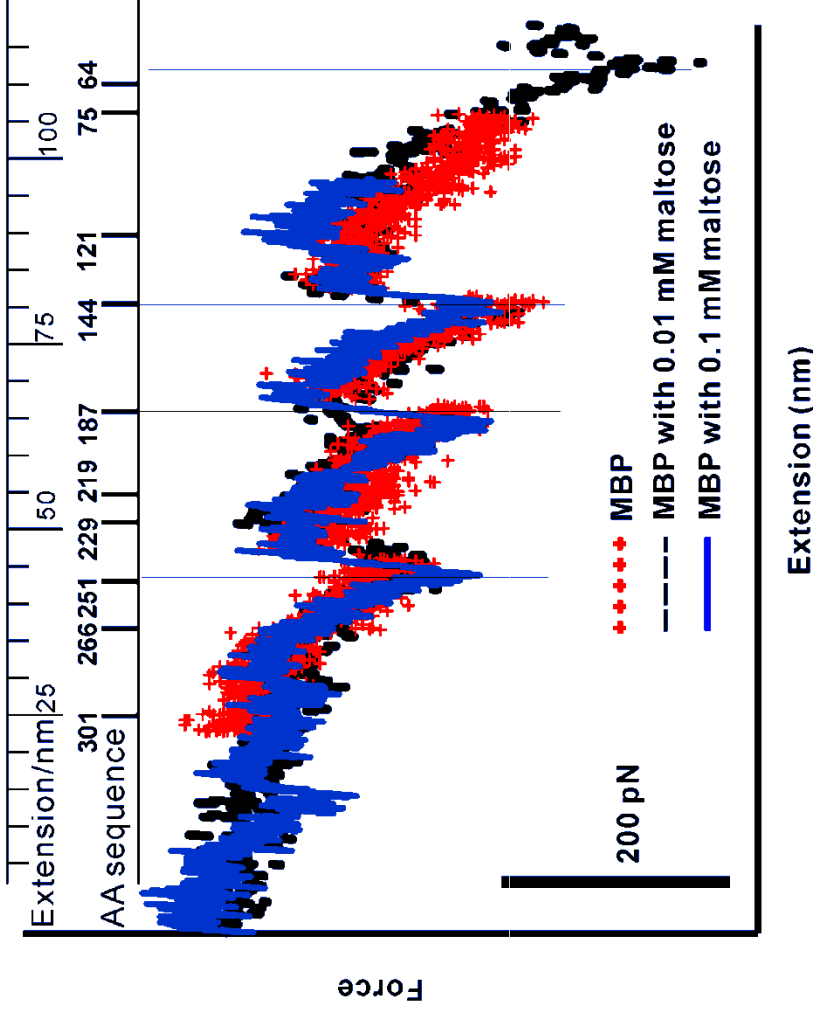


By reducing the pulling force of the cantilever, so-called fly-fishing mode, the protein molecule was allowed to relax and refold.

Fewer force transitions in refolding traces
 → slow refolding rate (fast mis-fold)
 → larger refolding barrier

The unfolded protein was relaxed to a small extension (dotted lines), resulting in elastic behavior that is typical of a simple, entropic spring-like, polymer chain. The protein molecule was allowed to relax 2 seconds, during which time it partially refolded back to its folded state. When stretched again, the refolded domains unfold again to produce the characteristic f-e traces, shown as relaxed proteins were monitored again (bottom solid lines).

Sequential Unfolding of MBP with Maltose



In the presence of maltose, the probability for the AFM tips to capture MBP at the His-tag end decreased by at least 50% → indicates that upon binding the ligand, MBP undergoes a conformational change which reduces accessibility of the C-terminal region.

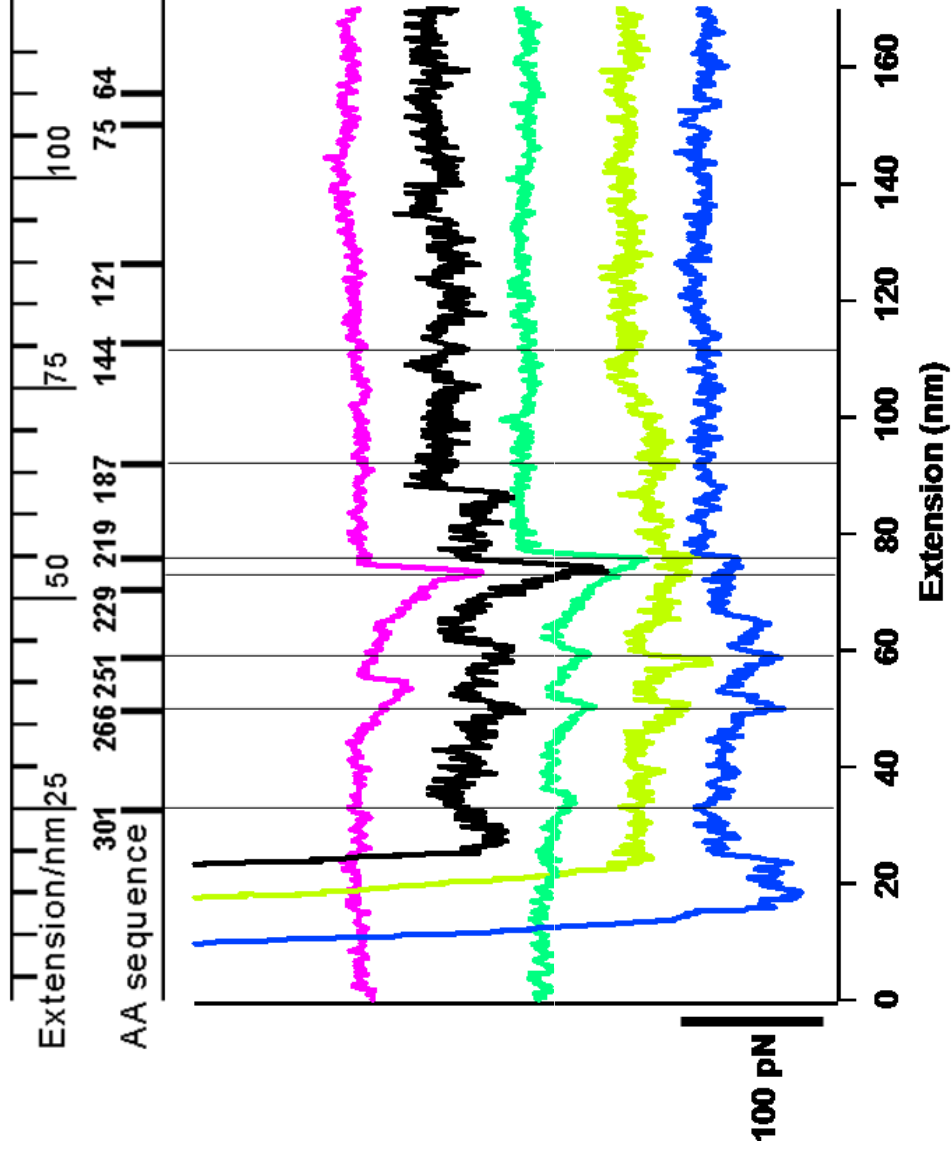
With and without ligands, MOST of the unfolding force transitions of MBP match with each other, indicating that the main unfolding barrier positions are not influenced by the ligand binding.

Noticed that our results CONTRAST those with recently reported optical tweezers data, where two-state behavior was observed.

?? a protein conformation bound to mica surface that disrupted protein folding or caused partial denaturation.

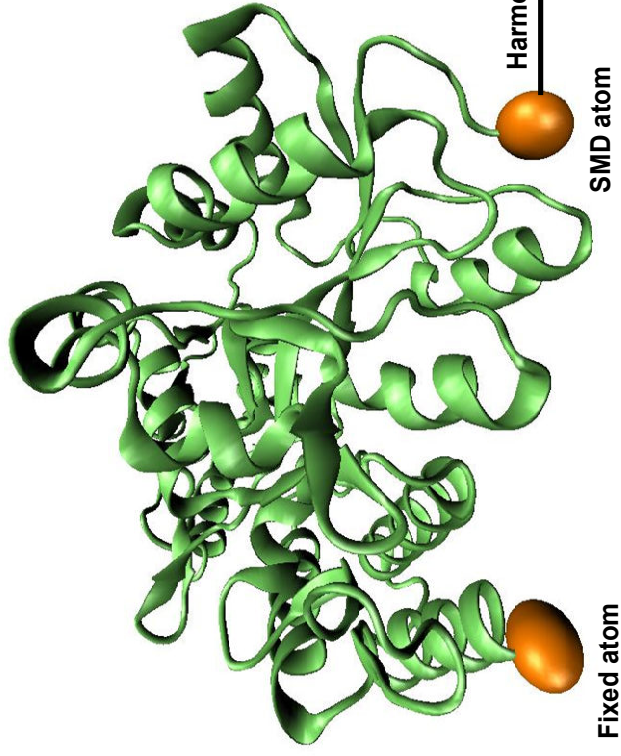
➔ Change sample surface!

Sequential Unfolding of MBP – on Gold Substrates



The **SAME** characteristic force transitions -- for negatively charged mica and amylose-gold substrates.

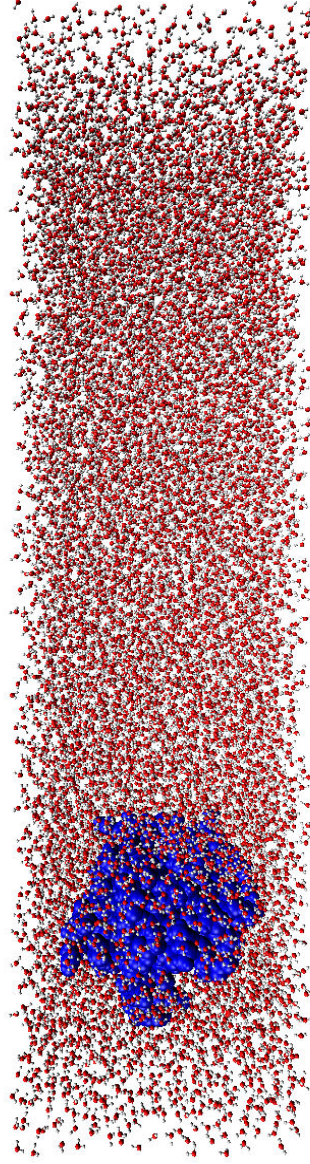
So that if surface binding caused significant unfolding, then an effect should have been observed. It seems likely that surface adsorption slows down unfolding (by reducing the reaction coordinate diffusion coefficient), allowing intermediate steps to be identified.

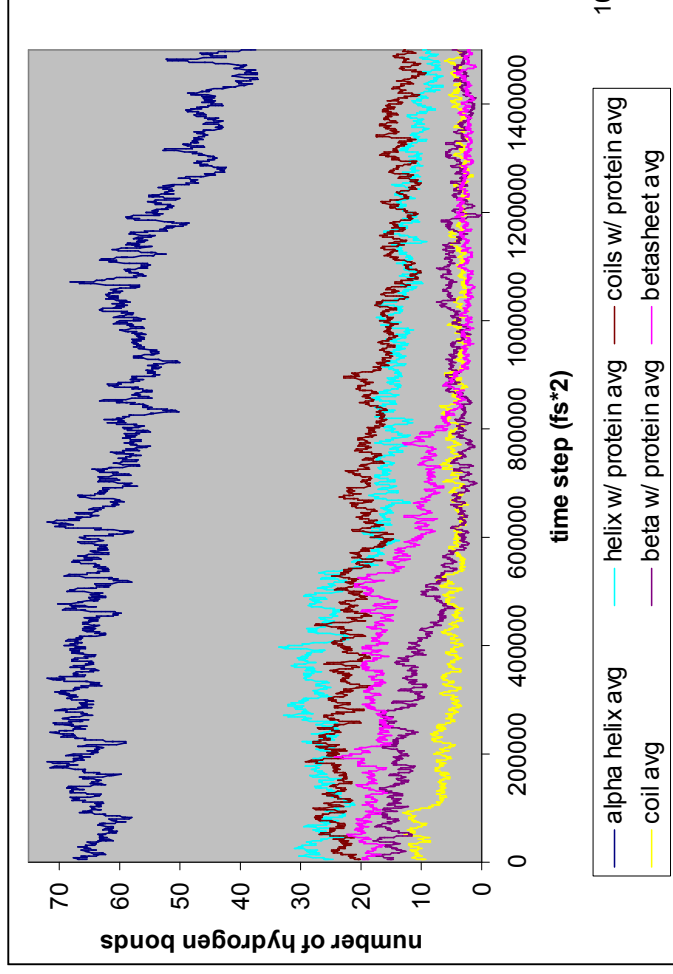


The setup of an SMD simulation. The SMD reference file determines which atoms are fixed in space and which ones are fixed to the moving restraint point (dummy atom) via a harmonic potential.

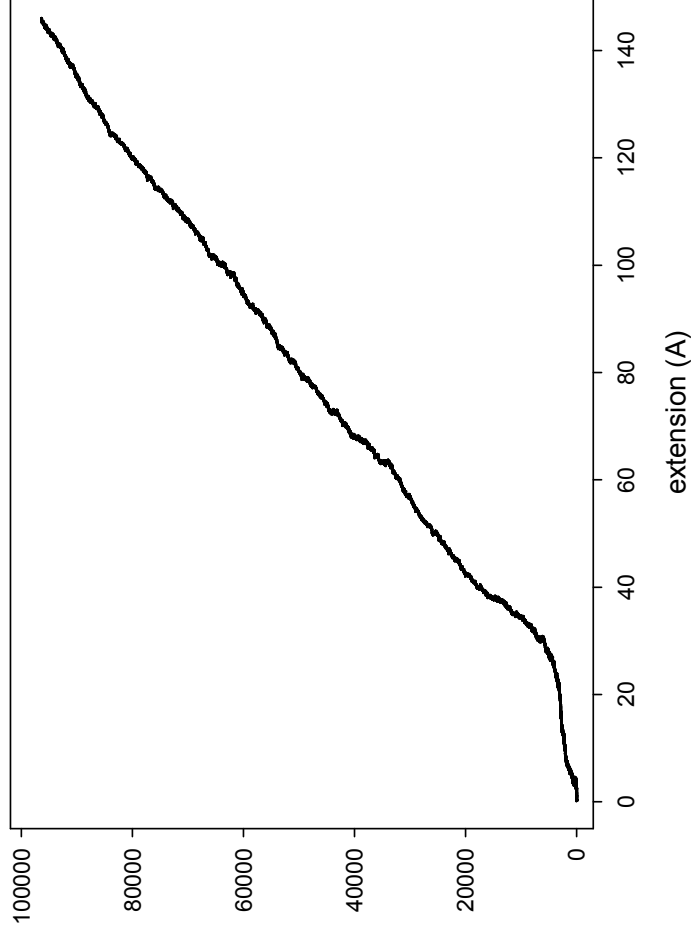
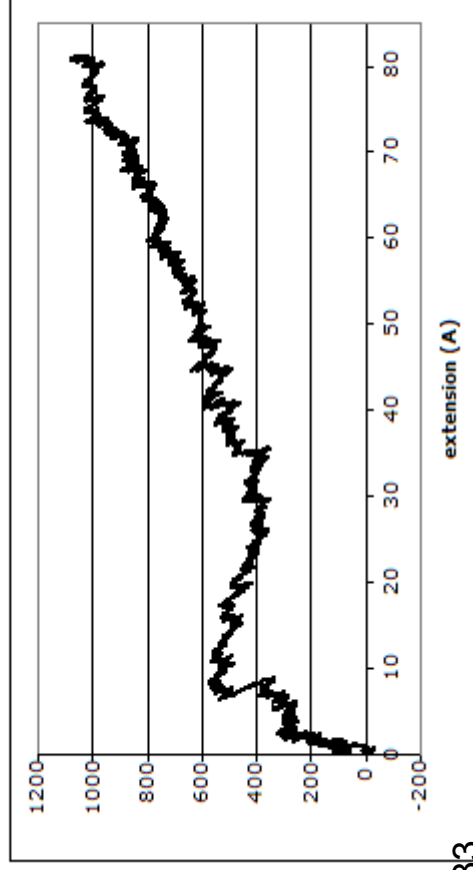
Setup for SMD

simulations. Water box in red, MBP-29 in blue. Total system size: 190 x 50 x 50 Å³ containing 39513 atoms. The pulling direction in this picture is towards the right.





force curve: pulling speed is 0.00015 A/fs with a k of 695 pN/nm. This is about 0.65 ns. The peak around 10 Å, corresponds to the separation of the pulled helix from the next one.



Calculation of the total work from the force extension curve.

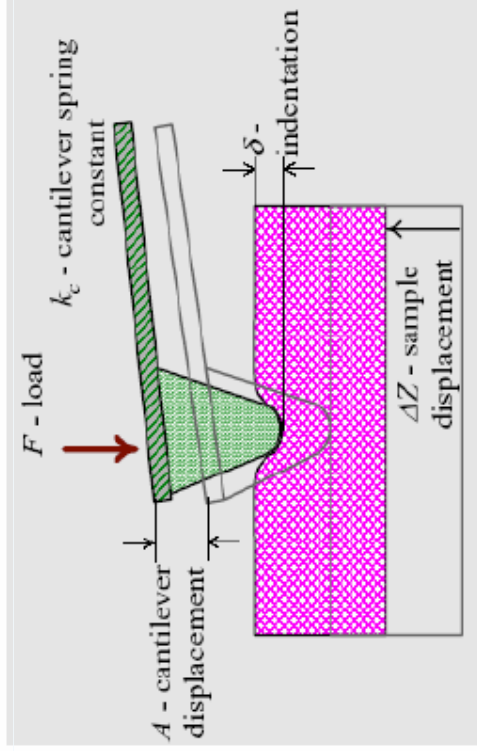
The Young modulus determination from Force-Distance curves

$F = kd$ (Hooke's law for the cantilever)
 $F \sim E \delta^\alpha$ (Hertz law for tip-surface contact)

$Z = d + \delta$

$\alpha = 2$ for cone/plane contact

$\alpha = 3/2$ for sphere/plane contact



Common problem of such measurements is large error in Z-position of the point of the tip-surface contact ($dF/dz=0$)

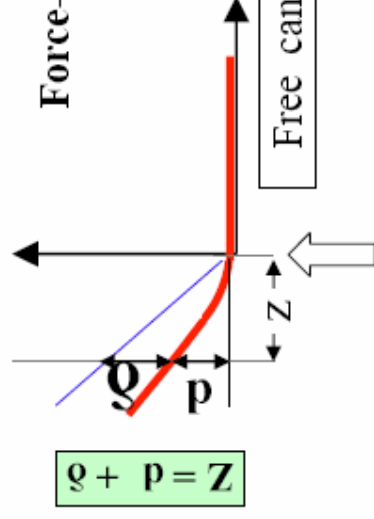
Deflection, d (=tip displacement)

Force-Distance plot for hard surface



Sample (piezo) displacement, z

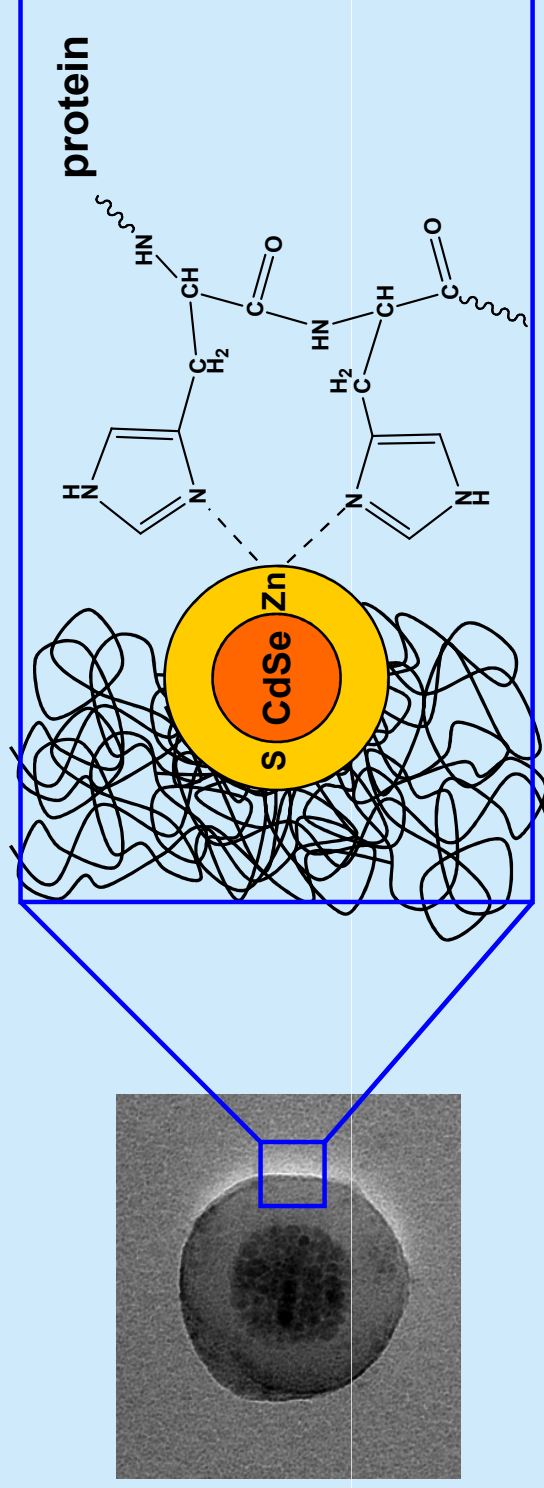
Force-Distance plot for soft surface



Piezo displacement (z) =
 tip displacement (d) + surface deformation (δ)

These are my probes
~100nm diameter

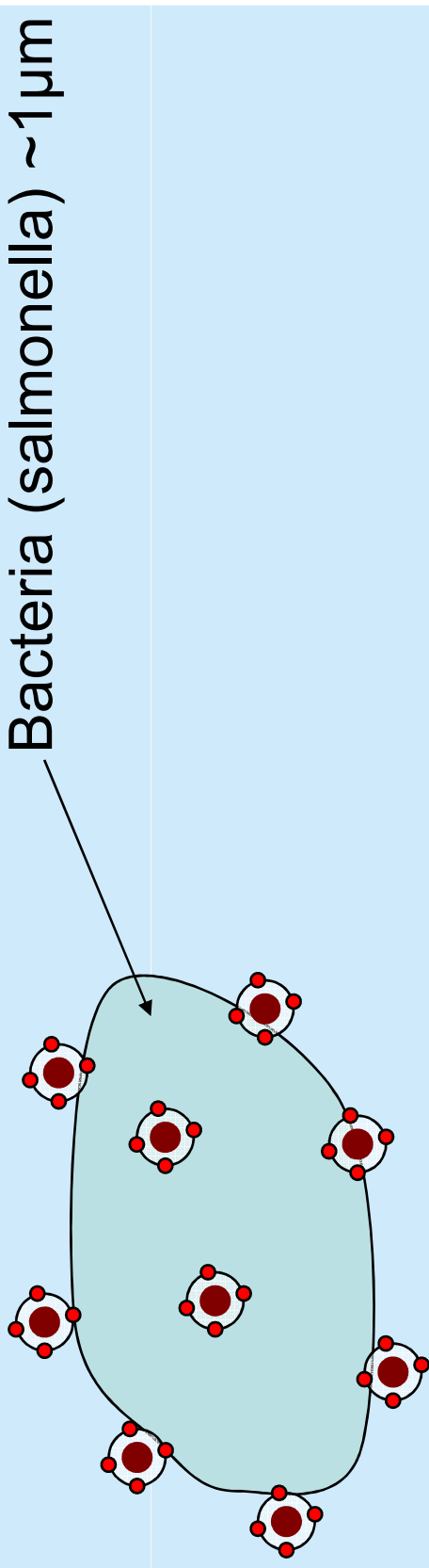
-QDs conjugated to proteins are deposited on the surface



is a schematic of the bacteria and nanoprobe conjugate

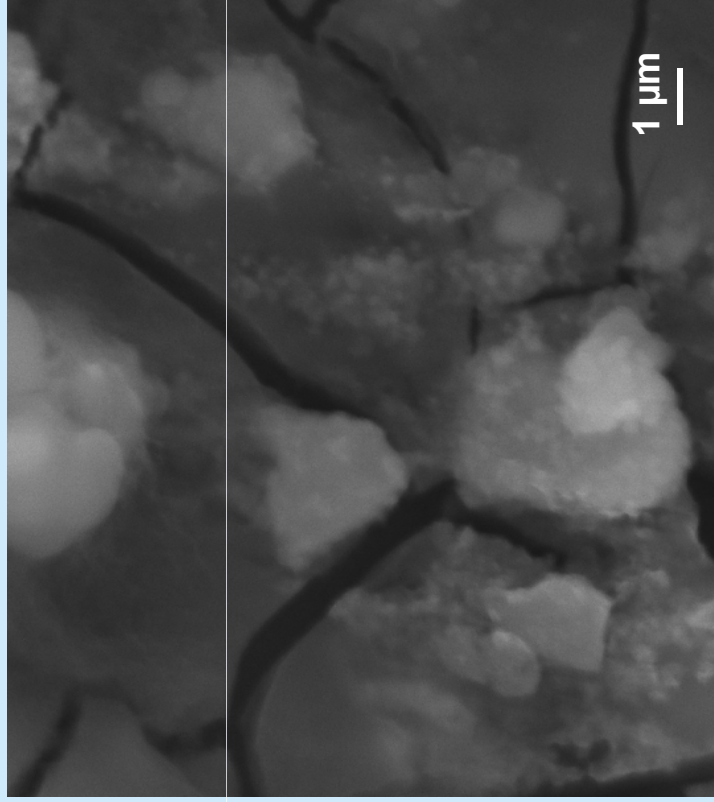
● Nanoprobe (polymer colloid) ~100nm

● QD+protein ~5-10nm

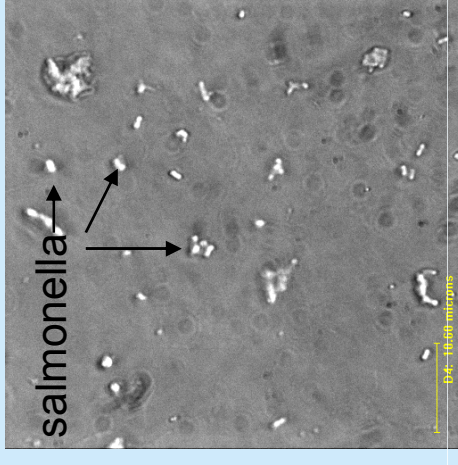


High-Resolution SEM images and optical/fluorescence images

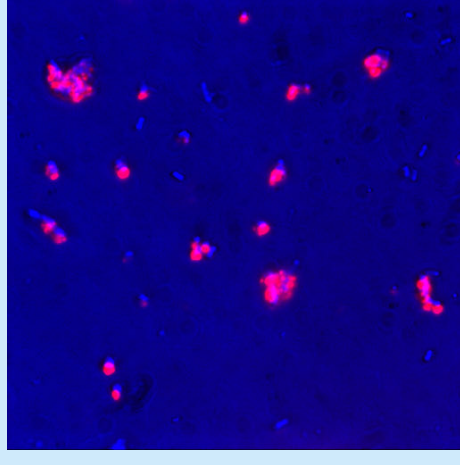
Salmonella-nanoprobe complex



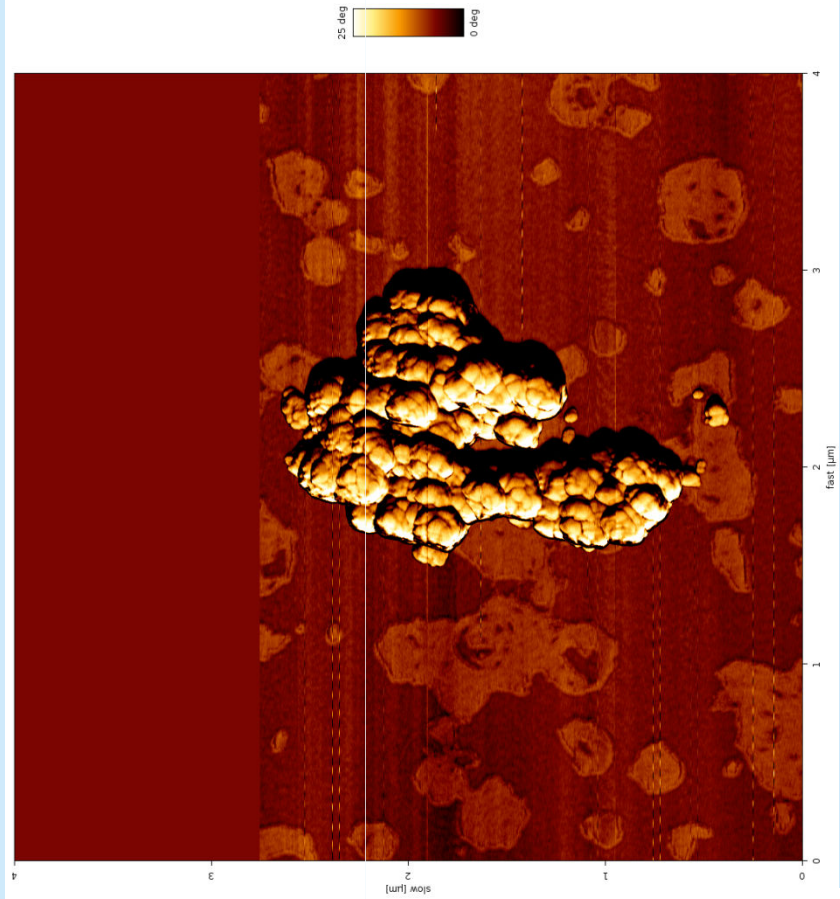
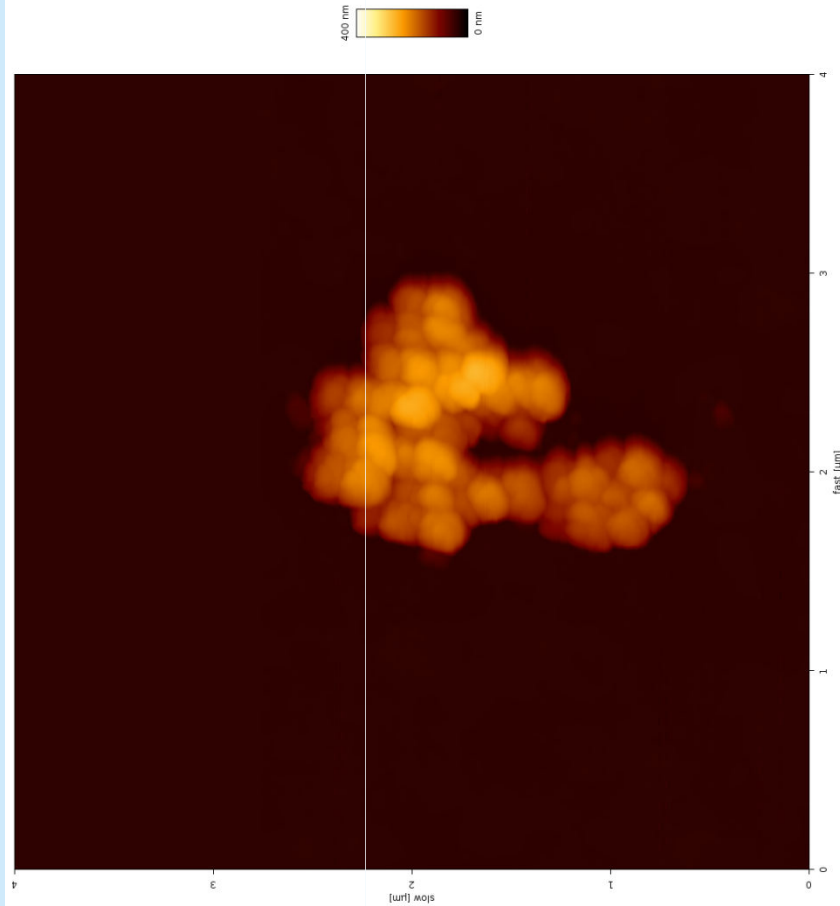
Optical Microscopy



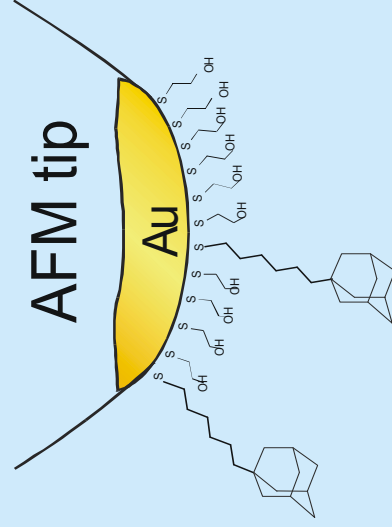
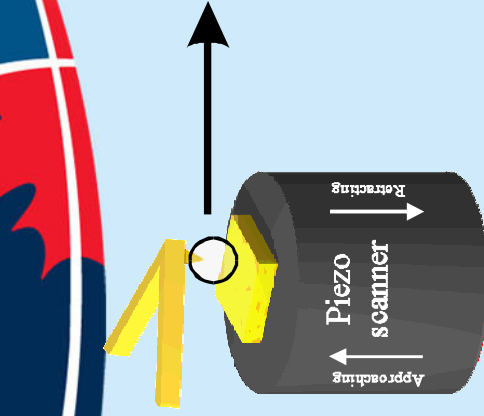
Transmission



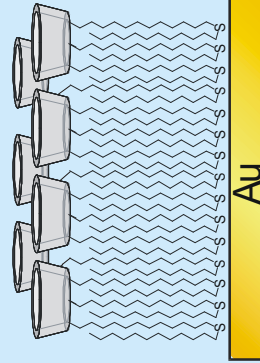
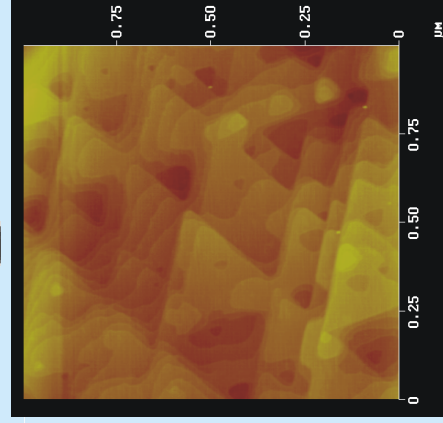
**Fluorescence-transmission
composite**



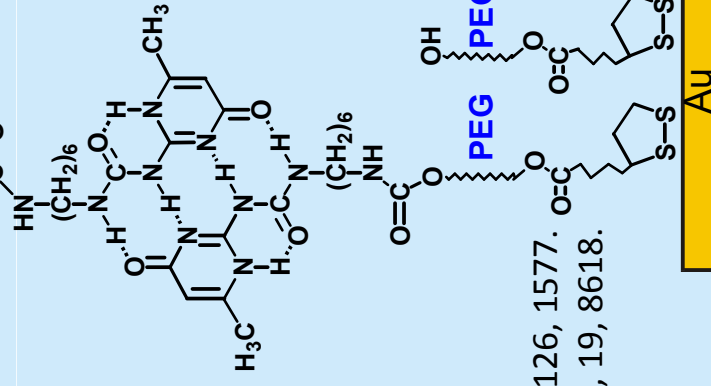
Stretching and Rupturing Individual Supramolecular Dimers and Polymers



Non-Equilibrium system:
Complexation constant:
 $K > 10^7 \text{ M}^{-1}$



Equilibrium system:
complexation constant:
 $K < 10^4 \text{ M}^{-1}$



- Auletta T; de Jong MR; Mulder A; van Veggel, FCJM; Huskens J; Reinhoudt DN;
Zou S; Zapotoczny S; Schönherr H; Vancso GJ; Kuipers L *J. Am. Chem. Soc.*, 2004, 126, 1577.
Zou, S.; Zhang, Z.; Förch, R.; Knoll, W.; Schönherr, H.; Vancso, G. J. *Langmuir*, 2003, 19, 8618.
Zou, S.; Schönherr, H.; Vancso, G. J. *Angew. Chem. Int. Ed.* 2005, 44, 956-959.
Zou, S.; Schönherr, H.; Vancso, G. J. *J. Am. Chem. Soc.*, 2005, 127, 11230.

Single Molecule Manipulation Techniques

Method	Force range (pN)	Dynamical range	Minimum displacement [nm]
Magnetic beads	0.01–100	> 1 s	10
Optical tweezers	0.1–150	> 10 ms	10
Microneedles	> 0.1	> 100 ms	1
BFP	0.5–1000	> 1 ms	10
AFM	> 1	> 1 μ s	0.1

Typical application:

Actin stretching,

unzipping and twisting DNA

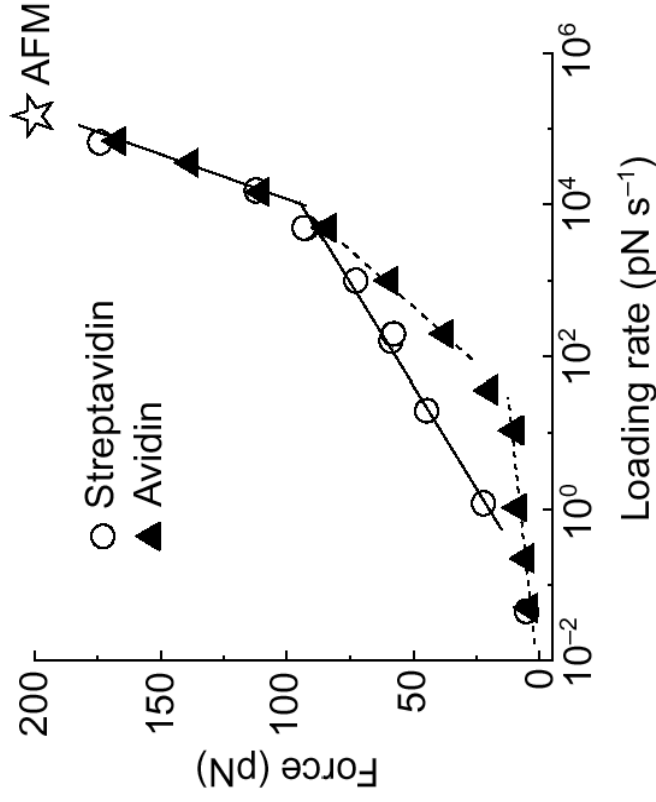
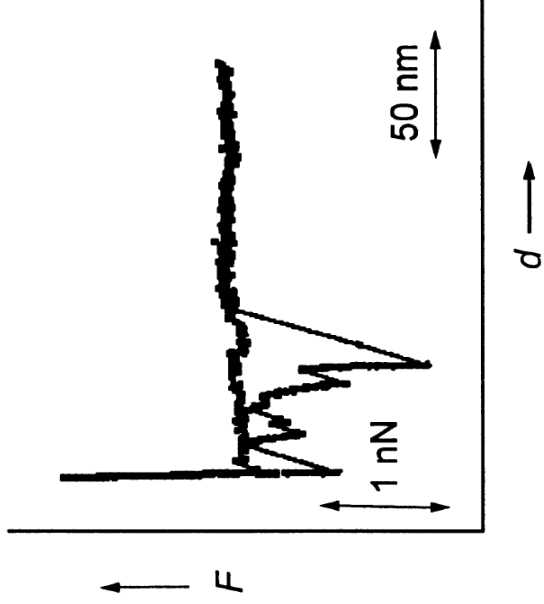
Membrane anchors, receptor–ligand pairs

Stretching of DNA, protein, polysaccharides, synthetic polymers

Loading Rate Dependent Single Molecule Force Spectroscopy

Force-induced rupture of double-stranded DNA.

* Lee, G. U.; Chrisey, L. A.; Colton, R. J. *Science* 1994, 266, 771.

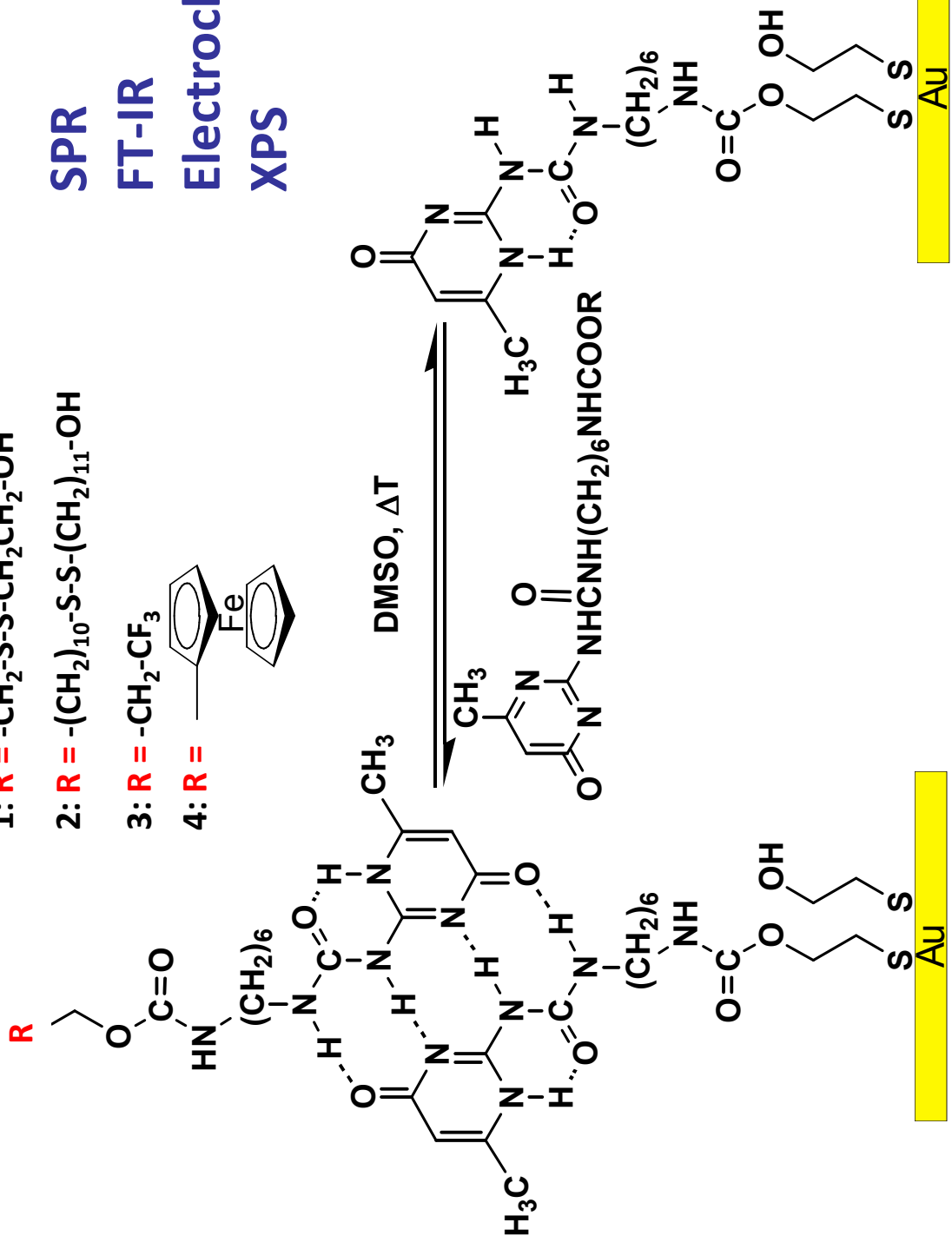
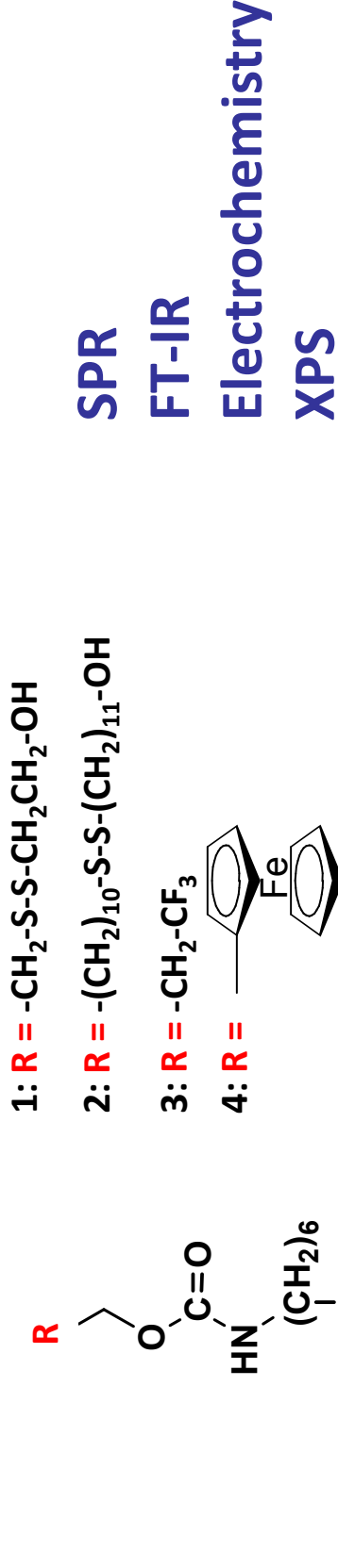


Biotin-avidin bond strengths.

* Florin, E. L.; Moy, V. T.; Gaub, H. E. *Science* 1994, 264, 415.

* Merkel, R.; Nassoy, P.; Leung, A.; Ritchie, K.; Evans, E. *Nature*, 1999, 397, 50-53.

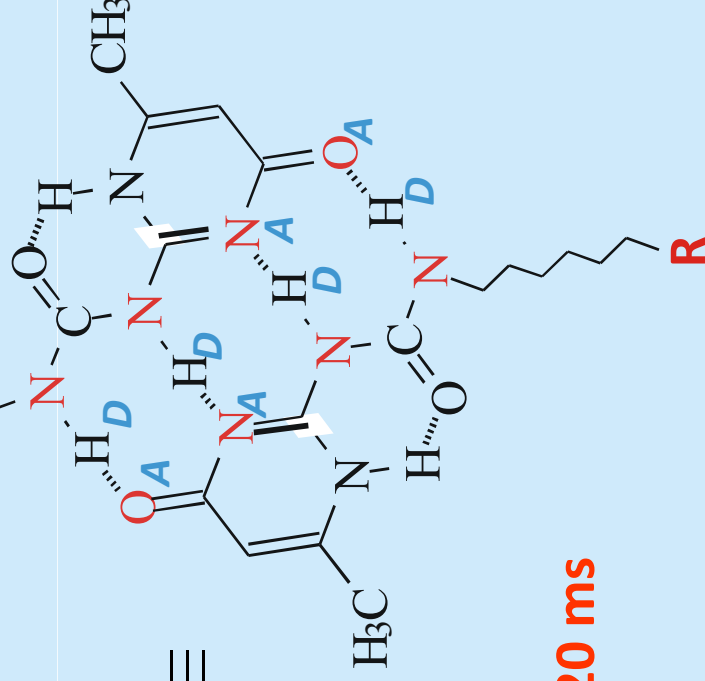
Quadruple Hydrogen Bonding System at Surfaces



Supramolecular Polymers



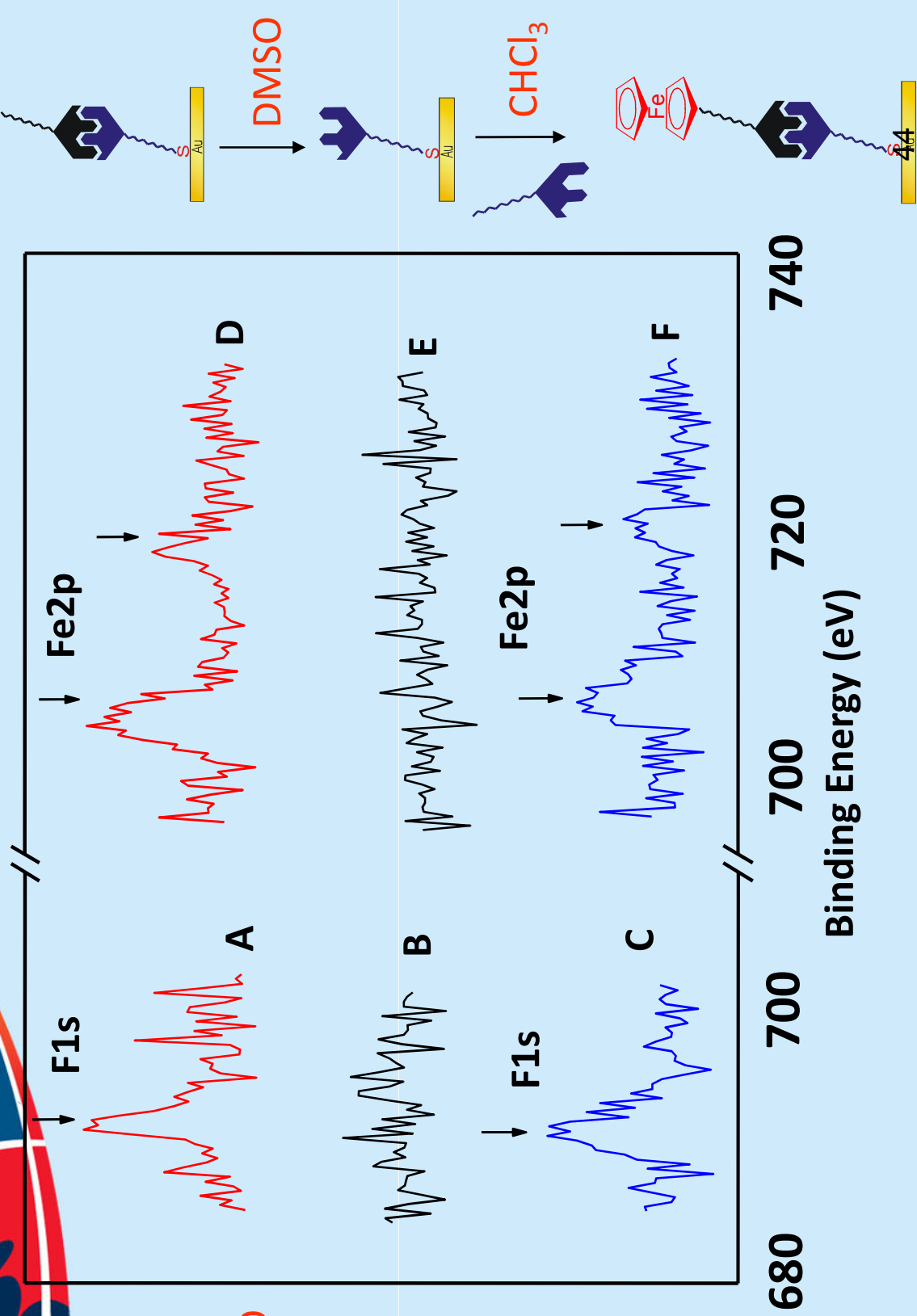
Supramolecular Polymers



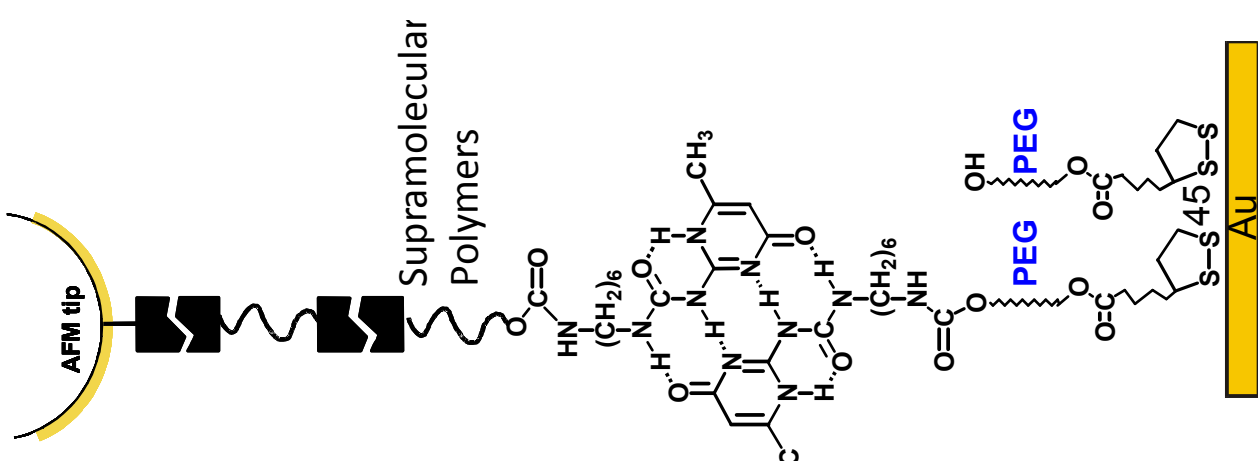
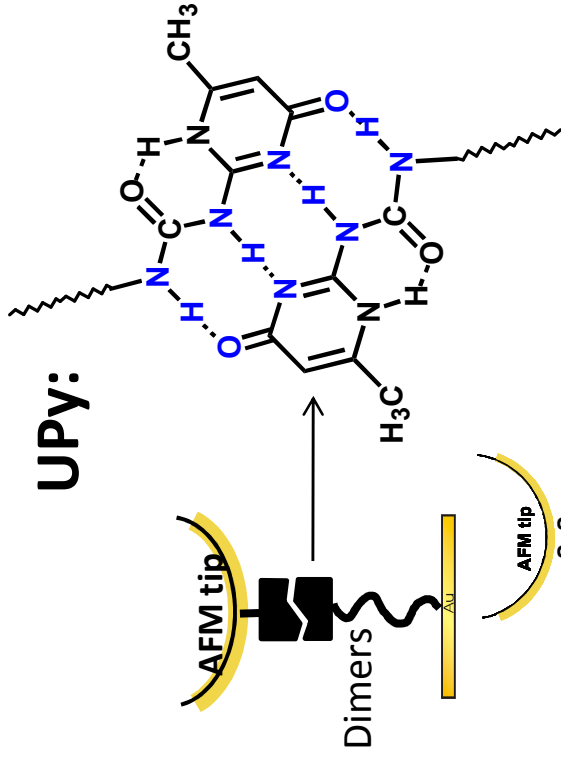
RT: $K < 51 \text{ M}^{-1}$ in DMSO

$K > 10^7 \text{ M}^{-1}$ in CHCl_3 , Life time: $> 120 \text{ ms}$

XPS Evidence for Molecular Recognition



H-bonding UPy Complex on Surface



- self-complementary molecular recognition of UPy moieties mediated by quadruple hydrogen bonding sites -- SAMs of UPy disulfide adsorbates on gold-
- dimerization constant can be tuned by solvent and T-
- characterized by XPS, SPR, DPV, AFM, FT-IR –

-Langmuir, 2003, 19, 8618.

- H-bonding complexes immobilized on surfaces
- Unbinding forces of UPy complex: $\sim 180 \pm 21$ pN at loading rate: ~ 35 nN/s
- Stretching individual reversible supramolecular polymer chains
- Rupture force \sim loading rate dependent

Angew. Chem. Int. Ed. 2005, 44, 956-959.

J. Am. Chem. Soc., 2005, 127, 11230.